PB83-122671

Mathematical Model, SERATRA, for Sediment-Contaminant Transport in Rivers and Its Application to Pesticide Transport in Four Mile and Wolf Creeks in Iowa

Battelle Pacific Northwest Labs.
Richland, WA

Prepared for

Environmental Research Lab.
Athens, GA

Aug 82

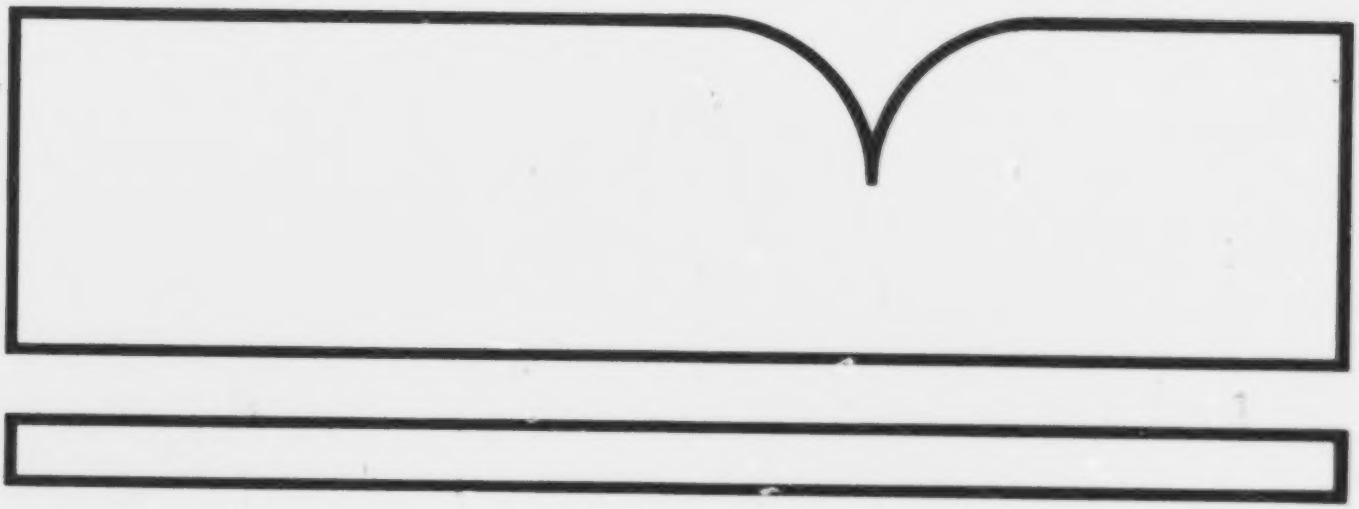

U.S. Department of Commerce
National Technical Information Service
NTIS

United States
Environmental Protection
Agency

Environmental Research
Laboratory
Athens GA 30613

EPA-600/3-82-045
August 1982

Research and Development

PB83-122671

EPA

Mathematical Model, SERATRA, for Sediment-Contaminant Transport in Rivers and Its Application to Pesticide Transport in Four Mile and Wolf Creeks in Iowa

REPRODUCED BY
NATIONAL TECHNICAL
INFORMATION SERVICE
U.S. DEPARTMENT OF COMMERCE
SPRINGFIELD, VA 22161

TECHNICAL REPORT DATA
(Please read Instructions on the reverse before completing)

1. REPORT NO. EPA-600/3-82-045	2. Applications Guide
3. RECIPIENT'S ACCESSION NO. PB83 122671	
4. TITLE AND SUBTITLE Mathematical Model, SERATRA, for Sediment-Contaminant Transport in Rivers and Its Application to Pesticide Transport in Four Mile and Wolf Creeks in Iowa	5. REPORT DATE August 1982
	6. PERFORMING ORGANIZATION CODE
7. AUTHOR(S) Y. Onishi and S.E. Wise	8. PERFORMING ORGANIZATION REPORT NO.
9. PERFORMING ORGANIZATION NAME AND ADDRESS Battelle Pacific Northwest Laboratories Richland, Washington 99352	10. PROGRAM ELEMENT NO. AARB1A
	11. CONTRACT/GRANT NO. 68-03-2613
12. SPONSORING AGENCY NAME AND ADDRESS Environmental Research Laboratory--Athens GA Office of Research and Development U.S. Environmental Protection Agency Athens, Georgia 30613	13. TYPE OF REPORT AND PERIOD COVERED Final, 4/78-1/80
	14. SPONSORING AGENCY CODE EPA/600/01
15. SUPPLEMENTARY NOTES	

16. ABSTRACT

The sediment-contaminant transport model SERATRA was used as an integral part of the Chemical Migration and Risk Assessment (CMRA) Methodology, which simulates migration and fate of a contaminant over the land surface and in receiving streams, to assess potential short- and long-term impact on aquatic biota. SERATRA, an unsteady, two-dimensional (longitudinal and vertical) finite element model, consists of three submodels coupled to include the effects of sediment-contaminant interactions--a sediment transport submodel, a dissolved contaminant transport submodel, and a particulate contaminant (contaminants adsorbed by sediment) transport submodel. The sediment transport submodel simulates transport, deposition and scouring of three sediment size fractions of cohesive and noncohesive sediments. The dissolved contaminant transport submodel includes mechanisms of contaminant adsorption/desorption and contaminant degradation resulting from hydrolysis, oxidation, photolysis, volatilization, biological activities and radionuclide decay to predict migration of dissolved contaminant. The particulate contaminant submodel simulates transport, deposition and scouring of contaminants associated with three size fractions of sediments. SERATRA also predicts changes of bed conditions for sediment and particulate contaminants.

17. KEY WORDS AND DOCUMENT ANALYSIS

a. DESCRIPTORS	b. IDENTIFIERS/OPEN ENDED TERMS	c. COSATI Field/Group

18. DISTRIBUTION STATEMENT RELEASE TO PUBLIC	19. SECURITY CLASS (This Report) UNCLASSIFIED	21. NO. OF PAGES 70
	20. SECURITY CLASS (This page) UNCLASSIFIED	22. PRICE

EPA Form 2220-1 (9-73)

EPA 600/3-82-045
August 1982

MATHEMATICAL MODEL, SERATRA, FOR SEDIMENT-CONTAMINANT TRANSPORT IN RIVERS AND ITS APPLICATION TO PESTICIDE TRANSPORT IN FOUR MILE AND WOLF CREEKS IN IOWA

by

Y. Onishi and S.E. Wise

Battelle
Pacific Northwest Laboratories
Richland, Washington 99352

Contract No. 68-03-2613

Project Officer

Robert B. Ambrose
Technology Development and Applications Branch
Environmental Research Laboratory
Athens, Georgia 30613

ENVIRONMENTAL RESEARCH LABORATORY
OFFICE OF RESEARCH AND DEVELOPMENT
U.S. ENVIRONMENTAL PROTECTION AGENCY
ATHENS, GEORGIA 30613

NOTICE

Mention of trade names or commercial products does not consititute endorsement or recommendation for use.

FOREWORD

As environmental controls become more costly to implement and the penalties of judgment errors become more severe, environmental quality management requires more efficient management tools based on greater knowledge of the environmental phenomena to be managed. As part of this Laboratory's research on the occurrence, movement, transformation, impact, and control of environmental contaminants, the Technology Development and Applications Branch develops management and engineering tools to help pollution control officials achieve water quality goals through watershed management.

Many toxic contaminants are persistent and undergo complex interactions in the environment. As an aid to environmental decision-makers, the Chemical Migration and Risk Assessment Methodology was developed to predict the occurrence and duration of pesticide concentrations in surface waters receiving runoff from agricultural lands and to assess potential acute and chronic damages to aquatic biota.

David W. Duttweiler
Director
Environmental Research Laboratory
Athens, Georgia

ABSTRACT

The sediment-contaminant transport model SERATRA was used as an integral part of the Chemical Migration and Risk Assessment (CMRA) Methodology, which simulates migration and fate of a contaminant over the land surface and in receiving streams, to assess potential short- and long-term impact on aquatic biota. SERATRA, an unsteady, two-dimensional (longitudinal and vertical) finite element model, consists of three submodels coupled to include the effects of sediment-contaminant interactions--a sediment transport submodel, a dissolved contaminant transport submodel, and a particulate contaminant (contaminants adsorbed by sediment) transport submodel. The sediment transport submodel simulates transport, deposition and scouring of three sediment size fractions of cohesive and noncohesive sediments. The dissolved contaminant transport submodel includes mechanisms of contaminant adsorption/desorption and contaminant degradation resulting from hydrolysis, oxidation, photolysis, volatilization, biological activities and radionuclide decay to predict migration of dissolved contaminant. The particulate contaminant submodel simulates transport, deposition and scouring of contaminants associated with three size fractions of sediments. SERATRA also predicts changes of bed conditions for sediment and particulate contaminants.

SERATRA was applied to Four Mile and Wolf Creeks in Iowa to simulate transport of sediment and the pesticide alachlor in these streams. Study results demonstrate that SERATRA is a useful tool for evaluating migration and fate of various hazardous dubstances and toxic chemicals in rivers by including contaminant interaction and contaminant degradation.

Companion reports to this document are Methodology for Overland and Instream Migration and Risk Assessment of Pesticides, User's Manual for the Instream Sediment-Contaminant Transport Model SERATRA, User's Manual for EXPLORE-I: A River Basin Water Quality Model (Hydrodynamic Module Only), and Frequency Analysis of Pesticide Concentrations for Risk Assessment (FRANCO Model).

This report was submitted in partial fulfillment of Contract No. 68-03-2613 by Battelle Pacific Northwest Laboratories under the sponsorship of the U.S. Environmental Protection Agency. This report covers the period April 1978 to January 1980, and work was completed as of January 1980.

CONTENTS

ABSTRACT iv

FIGURES vii

LIST OF SYMBOLS ix

1. INTRODUCTION 1

2. CONCLUSIONS 3

3. FORMULATION OF MODEL, SERATRA 4

3.1 SEDIMENT TRANSPORT SUBMODEL 4

3.2 DISSOLVED CONTAMINANT TRANSPORT SUBMODEL. . . 8

Chemical Degradation Due to Hydrolysis . . . 11

Hydrolysis 11

Chemical Degradtion Due to Oxidation . . . 11

Chemical Degradation Due to Photolysis . . . 12

Chemical-Degradation Due to Volatilization . . 13

Biodegradation 14

3.3 PARTICULATE CONTAMINANT TRANSPORT MODEL. . . 14

3.4 FINITE ELEMENT TECHNIQUE 16

Galerkin Weighted Residual Method 17

Finite-Element Equations 18

Time-Dependent Solution 20

3.5 LISTS OF INPUT DATA AND SIMULATION OUTPUT . . 21

4. MODEL APPLICATION RESULTS 23

CASE 1. CALIBRATION RUN 27

CASE 2. THREE-YEAR SIMULATION RUN 30

REFERENCES. 54

LISTS OF FIGURES

1 Four Mile and Wolf Creeks in Iowa 24

2 Time variations of simulated concentration of sand, silt, clay and total sediment at Four Mile Creek River kilometer 2.5 28

3 Time variations of simulated particulate alachlor concentrations associated with sand, silt and clay, together with mean particulate alachlor concentrations at Four Mile Creek River kilometer 2.5 29

4 Time variations of simulated dissolved, particulate and total alachlor concentrations at Four Mile Creek River kilometer 2.5 31

5 Vertical distributions of simulated sediment concentrations at Four Mile Creek River kilometer 2.5 at 12:00 p.m., July 10, 1971 32

6 Vertical distributions of simulated particulate alachlor adsorbed by sediments at Four Mile Creek River kilometer 2.5 at 12:00 p.m., July 10, 1971 33

7 Vertical distributions of simulated dissolved, particulate and total alachlor concentrations at Four Mile Creek River kilometer 2.5 at 12:00 p.m., July 10, 1971 34

8 Time variation of predicted flow rate at Wolf Creek River kilometer 5 during the three-year simulation period . . 35

9 Time variation of predicted total sediment concentration at Wolf Creek River kilometer 5 during the three-year simulation period 36

10 Time variation of predicted particulate alachlor concentration per unit weight of sediment at Wolf Creek River kilometer 5 during the three-year simulation period 37

11 Time variation of predicted particulate alachlor concentration per unit volume of water at Wolf Creek River kilometer 5 during the three-year simulation period 38

12 Time variation of predicted dissolved alachlor concentration at Wolf Creek River kilometer 5 during the three-year simulation period 39

13 Time variation of predicted total alachlor concentration at Wolf Creek River kilometer 5 during the three-year simulation period 40

14 Time variation of simulated flow rate at Wolf Creek River kilometer 5 during May 5, 1972 to August 15, 1972 . . . 41

15 Time variation of simulated total sediment concentration at Wolf Creek River kilometer 5 during May 5, 1972 to August 15, 1972 42

16 Time variation of simulated particulate alachlor concentration per unit weight of sediment at Wolf Creek River kilometer 5 during May 5, 1972 to August 15, 1972 43

17 Time variation of simulated total alachlor concentration at Wolf Creek River Kilometer 5 during May 5, 1972 to August 15, 1972 44

18 Time variation of simulated flow rate at Wolf Creek River kilometer 5 during May 26, 1973 to July 15, 1973 . . . 45

19 Time variation of simulated total sediment concentration at Wolf Creek River kilometer 5 during May 26, 1973 to July 15, 1973 46

20 Time variation of simulated particulate alachlor concentration at Wolf Creek River kilometer 5 during May 26, 1973 to July 15, 1973 47

21 Time variations of simulated particulate, dissolved and total alachlor concentrations at Wolf Creek River kilometer 5 duing May 30, 1973 to June 9, 1973 . . . 48

22 Longitudinal distribution of total sediment concentration at 6 a.m., July 4, 1973 49

23 Longitudinal distributions of simulated dissolved, particulate and total alachlor at 6 a.m., June 4, 1973 50

24 Variations of simulated particulate alachlor in the top bed layer accumulated during the three-year simulation period . 51

SYMBOLS

A = the river surface area

a = coefficient in Equation (34)

B = river width

$[B]$ = biomass per unit volume

b = coefficient in Equation (34)

$\bar{C}$ = average sediment concentration above water depth Z

C_j = concentration of sediment of jth size fraction

C_{ij} = sediment concentration of horizontal inflow for jth size fraction

$D = \frac{\epsilon_z}{\Delta z^2}$ in Equation (53)

d = flow depth

d_O = molecular diameters of oxygen

D_j = diameter of jth sediment

d_s = molecular diameter of contaminant

x^{e_i} = subdomain of interest in Equation (32)

f_{sj} = fraction of contaminant sorbed by jth sediment

f_w = fraction of contaminant left in solution

G_{Bj} = particulate contaminant concentration per unit weight of sediment on the river bed for jth sediment size fraction

G_j = particulate contaminant concentration per unit weight of sediment in jth sediment size fraction

G_{ij} = particulate contaminant concentration per unit weight of sediment in jth sediment size fraction in horizontal inflow

G_w = dissolved contaminant concentration

G_{wi} = dissolved contaminant concentration in horizontal inflow

h = water depth

i = element's number counted from the river bottom

$I_{o\lambda}$ = incident light intensity of wave length λ

I_λ = light intensity of wave length λ at water depth z

J = conversion constant in Equation (19)

K_1 = light attenuation coefficient for water

K_2 = light attenuation coefficient clue to suspended sediment in water

K_A = acid hydrolysis rate

K_{AB} = oxidation rate of free radical oxygen of [RO•]

K_B = base hydrolysis rate

K_{B1} = the second order rate constant for biodegradation

K_{bj} = transfer rate of contaminant with jth non-moving bed sediment

K_{C1} = the first order degradation rate due to hydrolysis

K_{C2} = the first order degradation rate due to oxidation

K_{C3} = the first order degradation rate due to photolysis

K_{C4} = the first order degradation rate due to volatilization

K_{C5} = the first order degradation rate due to biological activities

K_{dj} = rate of adsorption (or desorption) between dissolved contaminant and sediment (suspended and bed load sediments) of jth size fraction

k_j = transfer rate of contaminant with jth sediment in motion

K_j' = an empirical constant in Equation(9)

K_N = neutrol hydrolysis rate

K_o = oxygen reaeration rate

K_{oz} = oxidation rate of free radical oxygen of $[RO_2\cdot]$

K_w = $[H^+]\cdot[OH^-] \doteq 10^{-14}$

$RO\cdot$ = free radical oxygen

$RO_2\cdot$ = free radical oxygen

z = longitudinal distance

M_j = erodibility coefficient for sediment of jth size fraction

M_j' = weight of jth sediment

n = the number of subdomains

N = number of sediment size fractions considered. In this study, N = 3 (sand, silt and clay)

Q_i = horizontal inflow discharge equal to $U_iB\Delta z$

Q = horizontal outflow discharge equal to $U_oB\Delta z$

Q_T = sediment transport capacity

Q_{Ta} = actual sediment transport rate

Q_v = vertical flow discharge equal to (WA)

R = a domain of interest in Equation (31)

S_{Dj} = sediment deposition rate per unit area for jth sediment size fraction

S_{Rj} = sediment erosion rate per unit area for jth sediment size fraction

t = time

U_o = horizontal outflow velocity

U_i = horizontal inflow velocity

u = mean velocity

u_* = shear velocity

v = coefficient in Equation (28)

v_i = value v at i-th node

$\bar{V}$ = $(v_i + 1/2\ v_{i+1})$ shown in Equation (54)

$\tilde{V}$ = $(1/2\ v_i + v_{i+1})$ shown in Equation (54)

V_w = volume of water

W = vertical flow velocity

W_i = weighting function in Equation (30)

W_j = weighting function in Equation (29)

W_{sj} = fall velocity of sediment particle of jth size fraction

z = vertical direction

$[P]$ = symmetric tridiagonal matrix in Equation (50)

$[\tilde{P}]$ = symmetric tridiagonal matrix in Equation (55)

$[\bar{P}]$ = symmetric tridiagonal matrix in Equation (57)

$\{R\}$ = load vector in Equation (50)

$\{\tilde{R}\}$ = load vector in Equation (55)

$\{\bar{R}\}$ = load vector in Equation (57)

$[S]$ = unsymmetric tridiagonal matrix in Equation (50)

$[\tilde{S}]$ = unsymmetric tridiagonal matrix in Equation (55)

$[\bar{S}]$ = unsymmetric tridiagonal matrix in Equation (57)

α = coefficient in Equation (28)

β = coefficient in Equation (28)

γ = coefficient, i.e., probability that particle settling to the bed is deposited

γ_j = specific weight of jth sediment

Δz = increment of vertical distance

ε_z = vertical diffusion coefficient

ε_z = coefficient in Equation (28)

ε_λ = molar extinction coefficient of light with the wave length λ

λ = decay rate of radioactive material

τ_b = bed shear stress

τ_{cDj} = critical shear stress for sediment deposition for jth sediment size fraction

τ_{cRj} = critical shear stress for sediment erosion for jth sediment size fraction

ϕ = quantum yield

ϕ = variable in Equation (28)

$\tilde{\phi}$ = approximation of ϕ shown in Equation (30)

$\dot{\phi}$ = time derivative of ϕ

$L[\phi]$ = residual error in Equation (28)

SECTION 1

INTRODUCTION

The environmental impact of hazardous substances and toxic chemicals is an increasingly important issue (EPA 1978, Onishi and Wise 1978, Tofflamire et al. 1979). Although considerable effort is being made to minimize the release of contaminants to receiving water bodies, the decision makers of both government and industries must have a sound basis for impact assessment.

Mathematical models supported by coordinated data collection programs can be useful tools in assessing migration and ultimate fate of contaminants in surface waters. In order to obtain accurate predictions of contaminant transport, mathematical models must include the major transport and fate mechanisms. These mechanisms include:

1. convection and diffusion/disperson of contaminants

2. chemical and biological degradation due to hydrolysis, oxidation, photolysis, volatilization and biological activities

3. interaction between sediment and contaminants, such as contaminant adsorption by sediment; contaminant desorption from sediment to water; transport of pariculate contaminant (those adsorbed by sediment); deposition of particulate contaminants to the river bed; and resuspension of particulate contaminant from the bed

4. contaminant contributions from point and nonpoint sources into the river system.

Contaminants (e.g., pesticides, radionuclides, heavy metals, and many toxic chemicals) with high distribution coefficients or contaminants in surface water with high suspended sediment concentration are, to a great extent, adsorbed by river sediments. Thus, otherwise dilute contaminants are concentrated. Contaminated sediments may be deposited on the river bed, becoming a long-term source of pollution through desorption and resuspension. Until recently, sediment-contaminant interaction was not included in most models because of the complex nature of sediment transport and contaminant adsorption/desorption mechanism (Norton et al. 1974, Leerdertse 1970, Onishi 1979).

In order to obtain more realistic predictions, the model SERATRA (Onishi et al. 1976; Onishi 1977; Onishi et al. 1979a) was modified to include all important mechanisms described above. The modified version of

SERATRA was used as an integrated part of the Chemical Migration and Risk Assessment (CMRA) Methodology for the overland and instream migration and risk assessment of pesticides (Onishi et al. 1979b,c). This report describes the formulation of SERATRA and its application results to Four Mile and Wolf Creeks in Iowa.

SECTION 2

CONCLUSIONS

The unsteady, two-dimensional (vertical longitudinal and vertical), sediment-contaminant transport model, SERATRA, was adopted to be an integrated part of the CMRA Methodology. SERATRA was then applied to Four Mile and Wolf Creeks in Iowa to examine its applicability and limitations in simulating pesticide migration in these streams. The main conclusions are summarized as follows:

1. Application of SERATRA to Four Mile and Wolf Creeks in Iowa confirms that SERATRA is capable of predicting migration and fate of pesticides in rivers.

2. SERATRA is general enough to be applicable to nontidal rivers, streams and narrow impoundments.

3. Because SERATRA continuously and simultaneously simulates sediment and contaminant transport and fate by including all important mechanisms, such as sediment-contaminant interaction and contaminant degradation, it is a useful tool for evaluating both short- and long-term migration and fate of pesticides and other contaminants (e.g., radionuclides, heavy metals and other toxic chemicals).

SECTION 3

FORMULATION OF MODEL, SERATRA

The SERATRA code utilizes the finite element computation method with the Galerkin weighted residual technique. It consists of three submodels coupled to include the effects of sediment-contaminant interaction. The submodels are: 1) a sediment transport submodel, 2) a dissolved contaminant transport submodel, and 3) a particulate contaminant (contaminants adsorbed by sediment) transport submodel. SERATRA not only calculates distributions of sediment and contaminant concentrations in water, but also predicts river bed conditions, including bed elevation change, distribution of each sediment size fraction within the bed, and distribution of particulate contaminant concentration in the river bed. The detailed model formulation is discussed below:

3.1 SEDIMENT TRANSPORT SUBMODEL

Since the movements and adsorption capacities of sediments vary significantly with sediment sizes, the sediment transport submodel solves the migration of sediment (transport, deposition and scouring) for three size fractions of cohesive and non-cohesive sediments.

The model includes the mechanisms of:

1. convection and diffusion/dispersion of sediments
2. fall velocity and cohesiveness
3. deposition on the river bed
4. resuspension from the river bed (bed erosion and armoring)
5. sediment contributions from tributaries and point and nonpoint sources into the system.

Sediment minerology and water quality effects are implicitly included through the above mentioned mechanisms 2, 3, and 4.

Mass conservation of sediment passing through the control volume leads to the following expression for the transport of sediments:

$$\frac{\partial}{\partial t}(C_j B \ell) + (U_o C_j B - U_i C_{ij} B) + \frac{\partial}{\partial z}\left\{C_j (W - W_{sj}) B \ell\right\}$$

rate of accumulation | horizontal convection | vertical convection

$$= \frac{\partial}{\partial z}\left(\varepsilon_z \frac{\partial C_j}{\partial z} B \ell\right) + \frac{1}{h}(S_{Rj} - S_{Dj}) \qquad j = 1, 2, \ldots, N \qquad (1)$$

vertical diffusion | sediment erosion or deposition

where[a]

B = river width

C_j = concentration of sediment of jth size fraction

C_{ij} = sediment concentration of horizontal inflow for jth size fraction

h = water depth

ℓ = longitudinal distance

N = number of sediment size fractions considered. In this study, N = 3 (i.e., sand, silt and clay)

S_{Dj} = sediment deposition rate per unit area for jth sediment size fraction

S_{Rj} = sediment erosion rate per unit area for jth sediment size fraction

t = time

U_i = horizontal inflow velocity

U_o = horizontal outflow velocity

W = vertical flow velocity

W_{sj} = fall velocity of sediment particule of jth size fraction

z = vertical direction

ε_z = vertical diffusion coefficient

The model neglects longitudinal diffusion and assumes lateral sediment concentrations to be uniform. However, the model does handle vertical variations of longitudinal velocity to cause some longitudinal dispersal of sediment.

(a) The symbols defined above remain the same throughout the report

Boundary conditions at the water surface ($z = h$) and river bed ($z = 0$) are:

$$W - W_{sj} C_j - \varepsilon_z \frac{\partial C_j}{\partial z} = 0 \qquad \text{at } z = h \qquad (2)$$

$$-(1 - \gamma) W_{sj} C_j - \varepsilon_z \frac{\partial C_j}{\partial z} = 0 \qquad \text{at } z = 0 \qquad (3)$$

where

γ = coefficient, i.e., probability that particle settling to the bed is deposited.

In this study, γ is assumed to be unity, that is, for the same flow condition all suspended sediment settling to the river bed will stay on the river bed without going into the flow again.

Sediment erosion and deposition rates, S_{Rj} and S_{Dj}, are also evaluated separately for each sediment size fraction because erosion and deposition characteristics are significantly different for cohesive and noncohesive sediments.

Erosion and deposition of noncohesive sediments are affected by the amount of sediment the flow is capable of carrying. For example, if the amount of sand being transported is less than the flow can carry for given hydrodynamic conditions, the river will scour sediment from the stream bed to increase the sediment transport rate. This occurs until the actual sediment transport rate becomes equal to the carrying capacity of the flow or until the available bed sediments are all scoured, whichever occurs first. Conversely, the river deposits sand if its actual sediment transport rate is above the flow's capacity to carry sediment. Sediment transport capacity of flow, Q_T in this model, was calculated by either the Toffaleti or the Colby formulas (Vanoni 1975). The computer program of the Colby method developed by Mahmood and Ponce (Mahmood and Ponce 1975) was used. The sediment transport capacity of flow, Q_T, was then compared with the actual amount of sand, Q_{Ta}, being transported in a river water. Hence:

$$S_{Rj} = \frac{Q_T - Q_{Ta}}{A} \qquad (4)$$

$$S_{Dj} = \frac{Q_{Ta} - Q_T}{A} \qquad (5)$$

where

A = the river bed surface area.

The availability of bed sediments to be resuspended was also examined to determine the actual amount of sediment erosion.

For sediment erosion and deposition rates of cohesive sediments (silt and clay), the following Partheniades (1962) and Krone (1962) formulas, respectively, were adoped in this study:

$$S_{Rj} = M_j \left(\frac{\tau_b}{\tau_{cRj}} - 1 \right) \tag{6}$$

$$S_{Dj} = W_{sj} C_j \left(1 - \frac{\tau_b}{\tau_{cDj}} \right) \tag{7}$$

where

M_j = erodibility coefficient for sediment of jth size fraction

τ_b = bed shear stress

τ_{cDj} = critical shear stress for sediment deposition for jth sediment size fraction

τ_{cRj} = critical shear stress for sediment erosion for jth sediment size fraction

Values of M_j, τ_{cDj} and τ_{cRj} must be determined by field and/or laboratory tests for a particular river regime. The model examines the availability of cohesive sediments in the river bed to determine the actual amount of sediment erosion.

When the fall velocity, W_{sj}, depends on sediment concentration and no aggregation occurs, the fall velocity could be assumed (Krone 1962):

$$W_{sj} = K_j^{\wedge} C_j^{4/3} \tag{8}$$

where

$K_j^{\wedge}$ = an empirical constant depending on the sediment type.

3.2 DISSOLVED CONTAMINANT TRANSPORT SUBMODEL

The dissolved contaminant transport submodel includes the mechanisms of:

1. Convection and diffusion/dispersion of dissolved contaminants (pesticides, radionuclides, and other toxic substances) within the river

2. Adsorption (uptake) of dissolved contaminants by sediments (suspended and bed sediments) or desorption from sediments into water

3. Degradation of dissolved contaminants due to hydrolysis, oxidation, volatilization, photolysis and biological activities

4. Radionuclide decay

5. Contributions of dissolved contaminants from point and nonpoint sources into the system.

Effects of water quality (e.g., pH, water temperature, salinity, etc.) and clay minerals are taken into account through changes in the distribution coefficients for adsorption and desorption, K_{dj}, k_{dj}, respectively. In this model, distribution coefficients for adsorption can be assigned to a value different from that of desorption to be able to handle not-completely-reversible adsorption/desorption processes. Mass conservation of dissolved contaminants may be expressed as:

$$\frac{\partial}{\partial t}(G_w B\ell) + (U_o G_w B - U_i G_{wi} B) + \frac{\partial}{\partial z}(WG_w B\ell)$$

rate of accumulation — horizontal convection — vertical convection

$$= \frac{\partial}{\partial z}\left(\varepsilon_z \frac{\partial G_w}{\partial z} B\ell\right) - \lambda G_w B\ell - \sum_{i=1}^{5} K_{Ci} G_w B\ell$$

vertical diffusion — radionuclide decay — chemical and biological degradation and volatilization

$$- \sum_j K_j (K_{dj} C_j G_w - G_j) B\ell - \sum_j K_j (K'_{dj} C_j G_w - G_j) B\ell$$

adsorption to moving sediment — desorption from moving sediment

$$- \sum_j \gamma_j (1\text{-POR}) D_j K_{bj} (K_{dj} G_w - G_{Bj}) - \sum_j \gamma_j (1\text{-POR}) D_j K'_{bj} (K'_{dj} G_w - G_{Bj})$$

adsorption to bed sediment — desorption from bed sediment

$j = 1, 2, 3$ (9)

It was assumed that a contaminant has the same distribution coefficient values K_{dj} or K'_{dj}, for the moving (suspended and bed load sediments) and not moving (bed sediment without any motion) jth sediment. However, these two types of sediments have two different transfer rates, K_j or K'_j and K_{bj} or K'_{bj}, as expressed in Equation 9.

In addition to the previously defined symbols:

D_j = diameter of jth sediment

G_{Bj} = particulate contaminant concentration per unit weight of sediment in jth sediment size fraction in river bed

γ_j = specific weight of jth sediment

G_w = dissolved contaminant concentration

G_{wi} = dissolved contaminant concentration in horizontal inflow

G_j = particulate contaminants concentration per unit weight of jth sediment

K_{Ci} = the first order reaction rate of contaminant degradation due to hydrolysis, oxidation, photolysis, volatilization and biological activities

K'_{bj} = transfer rate of contaminants with jth non-moving sediment in bed

k_{dj}, k'_{dj} = rate of adsorption and desorption between dissolved contaminant and sediment (suspended and bed load sediments) of jth size fraction, respectively

K_j, K'_j = transfer rate of contaminants for adosprtion and desorption, respectively with jth sediment in motion

λ = decay rate of radioactive material.

POR = porosity of bed sediment

The distribution coefficient, K_{dj} and K'_{dj}, is defined by:

$$K_{dj} \text{ and } K'_{dj} = \frac{f_{sj}/M'_j}{f_w/V_w} = \frac{f_{sj}}{f_w C_j} \qquad (10)$$

where

f_{sj} = fraction of contaminant sorbed by jth sediment

f_w = fraction of contaminant left in solution

M'_j = weight of jth sediment

V_w = volume of water

$$\frac{f_{sj}}{f_w} = \frac{C_j G_j}{G_w}$$

Hence Equation 10 may be rewritten as:

$$G_j = K_{dj} G_w \text{ or } G_j = K'_{dj} G_w \qquad (11)$$

The adsorption of contaminant by sediments or desorption from the sediments is assumed to occur toward an equilibrium condition with the transfer rate, K_j or K'_j (with the unit of reciprocal of time), if the particulate contaminant concentration differs from its equilibrium values as expressed in Equation 12. Longitudinal diffusion is considered to be negligible when compared to convection. Longitudinal dispersal of contaminants due to vertical variation of longitudinal velocity is, however simulated in this study.

Boundary conditions at the water surface and river bed are:

$$WG_w - \varepsilon_z \frac{\partial G_w}{\partial z} = 0 \qquad \text{at } z = h \qquad (12)$$

$$\varepsilon_z \frac{\partial G_w}{\partial z} = 0 \qquad \text{at } z = 0 \qquad (13)$$

One of the important mechanisms of transport and fate of contaminants is degradation of contaminants in an aquatic environment. The contaminant degradation includes both chemical and biological reactions. Major mechanisms of chemical degradation are due to reactions of: 1) hydrolysis, 2) oxidation, and 3) photolysis (Smith et al. 1977). Due to lack of a present knowledge on degradation and volatilization of particulate contaminants (Smith et al. 1977), these degradation mechanisms were considered only for the dissolved contaminants. These degradation rates are included in Equation 9 as the first order kinetic reaction rates, K_{Ci}; i=1, 2, 3, 4 and 5. Actual formulations of chemical and biological degradation were obtained from pesticide studies conducted by Smith et al. 1977, Zepp and Cline 1977 and Falco et al. 1976. These formulations will be discussed below:

Chemical Degradation Due to Hydrolysis:

The fundamental concept of chemical reactivity is based on the quest to improve stability in the configuration of the outer shells. A contaminant in solution will react with other species in solution and form a complex if there is a large increase in stability. Hydrolysis reactions are a specialized type of complex formation in which the [OH^-] anion acts as the ligand. They are quite sensitive to pH changes. The rate of change of dissolved contaminant concentration due to hydrolysis is expressed by the following equation (Smith et al 1977):

Hydrolysis

$$-\frac{dG_w}{dt} = K_A\left[H^+\right]G_w + K_B\left[OH^+\right] GW + K_N G_w$$

$$= \left(K_A\left[H^+\right] + \frac{K_B K_w}{\left[H^+\right]} + K_N\right)G_w$$

$$= \left(K_A \cdot 10^{-pH} + K_B \cdot 10^{pH-14} + K_N\right)G_w$$

$$= K_{C1} G_w \qquad (14)$$

where

$$K_{C1} = K_A \cdot 10^{-pH} + K_B \cdot 10^{pH-14} + K_N$$

$$K_w = \left[H^+\right] \cdot \left[OH^-\right] \doteq 10^{-14}$$

$$pH = -\log\left[H^+\right]$$

K_A, K_B, K_N = acid, base and neutral hydrolysis rates; respectively

Rate coefficients, K_A, K_B and K_N can be determine laboratory tests (Smith et al. 1977).

Chemical Degradation Due to Oxidation

Oxidation of contaminants by free radical processes may become important under some environmental conditions. The rate of oxidation of contaminant may be expressed by the second order reactions depending on the concentration of free and radical oxygen and dissolved contaminant as shown below (Smith et al. 1977):

$$-\frac{dG_w}{dt} = K_{ox}\left[RO_2\cdot\right]G_w + K_{AB}\left[RO\cdot\right]G_w \qquad (15)$$

It is assumed that only a small concentration of dissolved contaminants is oxidized, and that the second term in the right hand side may be deleted (Smith et al. 1977). Hence:

$$-\frac{dG_w}{dt} = K_{ox}\left[RO_2\cdot\right]G_w = K_{C2}G_w \qquad (16)$$

where

K_{ox}, K_{AB} = oxidation rates of free radical oxygen of RO_2 and $\left[RO\cdot\right]$, respectively

$RO_2\cdot$ = free radical oxygen

$RO\cdot$ = free radical oxygen

The rate constant, K_{ox} can be obtained from laboratory tests outlined by Smith et al. (1977).

Chemical Degradation Due to Photolysis

Pesticides can be photochemically transformed by adsorbing light, expecially ultra violet light. The rate of contaminant concentration change due to photolysis reactions may be expressed by (Zepp and Cline 1977, Smith et al. 1977, and Stanford Research Institute 1979):

$$-\frac{dG_w}{dt} = \frac{2.303}{J}\,\phi \sum_{\lambda} \varepsilon_\lambda I_\lambda G_w \tag{17}$$

$$I_\lambda = I_{o\lambda} \exp\left\{-(K_1 + K_2 \bar{C})\,(h - z)\right\}$$

where

C = average sediment concentration above water depth Z

$I_{o\lambda}$ = incident light intensity of wave length λ

I_λ = light intensity of wave length λ at water depth Z

J = conversion constant

K_i = light attenuation coefficient for water

K_z = light attenuation coefficient due to suspended sediment in water

ε_λ = molar extinction coefficient of light with the wave length λ

ϕ = quantam yield

Since each computational cell has a vertical finite element thickness, the above equation was averaged over the element thickness for each element in this study. Hence:

$$-\frac{dG_w}{dt} = \frac{2.303}{J}\,\phi \sum_{\lambda} \varepsilon_\lambda I_o \exp\left[\left\{-(K_1 + K_2\bar{C})(n - i)\Delta z\right\} \cdot \left\{\frac{1 - \exp -(K_1 + K_2\bar{C})\Delta z}{(K_1 + K_2\bar{C})\,z}\right\}\right] G_w \tag{18}$$

$$= K_{C3} G_w$$

where

i = element's number counted from the river bottom

n = total number of elements

Δz = element thickness.

Various parameters and coefficients can be measured by conducting laboratory tests and/or field measurements (Zepp and Cline 1977, Smith et al. 1977, and Stanford Research Institute 1979).

Biodegradation:

A contaminant compound can be degraded by microbial activities in an aquatic environment. In this study it is assumed that microbial degradation can be expressed by the second order reaction (Falco et al. 1976, Smith et al. 1977) depending on concentrations of biomass and contaminant in water, as shown below:

$$-\frac{dG_w}{dt} = K_{B1}[B]G_w = K_{C5}G_w \tag{19}$$

[B] = biomass per unit volume

K_{B1} = the second order rate constant for biodegradation

Volatilization:

The volatilization of a contaminant occurs at the air-water interface. The change of contaminant concentration due to volatilization may be expressed by the following first order reaction (Smith et al. 1977):

$$-\frac{dG_w}{dt} = K_{C3}G_w \tag{20}$$

where

K_{C3} = volatilization rate of the contaminant

K_{C3} can be estimated by the following relationship:

$$(K_{C3})_{\text{water body}} = (K_o)_{\text{water body}}\left(\frac{K_{C3}}{K_o}\right)_{\text{laboratory test condition}}$$

$$= (K_o)_{\text{water body}}\left(\frac{d_o}{d_s}\right)$$

where

d_o, d_s = molecular diameters of oxygen and contaminant, respectively

(K_{C3}) laboratory test conditions = volatilization rate through any substances measure at a laboratory

(K_O) water = oxygen reaeration rate through water-air interfare

3.3 PARTICULATE CONTAMINANT TRANSPORT MODEL

The transport model of contaminants attached to sediment includes the mechanisms of:

1. Convection and diffusion/dispersion of particulate contaminants
2. Adsorption (uptake) of dissolved contaminants by sediments or desorption from sediments into water
3. Radionuclide decay
4. Deposition of particulate contaminants to the river bed or resuspension from the river bed
5. Contributions of particulate contaminants from point and nonpoint sources into the system.

As in the transport of sediments and dissolved contaminants, the conservation of contaminants adsorbed by each sand, silt and clay sediment may be expressed as:

$$\frac{\partial}{\partial t}(G_j B\ell) + (U_o G_j B - U_i G_{ij} B) + \frac{\partial}{\partial z}\left\{(W - W_{sj})G_j B\ell\right\} \qquad (21)$$

rate of accumulation — horizontal convection — vertical convection

$$= \frac{\partial}{\partial z}\left(\varepsilon_z \frac{\partial G_j}{\partial z} B\ell\right) - \lambda G_j B\ell + K_j (K_{dj} G_w - G_j) B\ell + K_j' (K_{dj}' G_w - G_j) B\ell + \frac{1}{h}(G_{Bj} S_R - G_j S_D$$

vertical diffusion — radionuclide decay — adsorption — desorption — contaminated sedime erosion and deposit

where

G_{ij} = particulate concentration per unit volume of water associated with the j_{th} sediment size fraction in horizontal inflow (no summation will be applied).

Longitudinal diffusion was assumed to be negligible, as compared to longitudinal convection. However, as noted before, the longitudinal dispersal of particulate contaminant due to nonuniform vertical distribution of longitudinal velocity is simulated in the model. It is also assumed that chemical and biological degradation of particulate

contaminants, except radionuclide decay, is not significant. However, if it is necessary to include these mechanisms, the radionuclide decay term can include them.

The boundary conditions at the water surface and bed are:

$$G_j (W - W_{sj}) - \varepsilon_z \frac{\partial G_j}{\partial z} = 0 \qquad \text{at } z = h \text{ and } 0 \tag{22}$$

The finite element technique with the Galerkin weighted residual method was used to solve transport equations of sediments, dissolved contaminants and particulate contaminants previously described.

3.4 FINITE ELEMENT TECHNIQUE

High speed digital computers have enabled engineers to employ various numerical discretization techniques for approximating solutions to complex mathematical equations. The finite element method is one such technique and has recently gained popularity for solving both linear and nonlinear partial differential equations.

Because of its increased solution accuracy and ready accommodation to various boundary geometrics (Desai and Abel 1972, Norton et al 1973, Onishi and Wise 1978) this method was used for this study. To apply the finite element method to a partial differential equation, an alternate integral equation is developed. The finite element method employing a Galerkin weighted residual is used to solve Equations 1, 9, and 21 with the boundary conditions of Equations 2, 3, 12, 13, and 22. Since the governing equations of sediment and contaminant transport have similar forms, the finite element technique is described here for the following convection- diffusion equation of the general form:

$$L\ \phi = \frac{\partial \phi}{\partial t} + \frac{\partial}{\partial z}(v\phi) - \frac{\partial}{\partial z}\left(\varepsilon_z \frac{\partial \phi}{\partial z}\right) + \alpha\phi - \beta \tag{23}$$

The coefficients v, ε_z, α, β are defined to accommodate the specific forms of the sediment and contaminant transport equations.

Galerkin Weighted Residual Method

The governing partial differential equation can be recast in an integral form employing the weighted residual method. This integral is formed by taking the product of $L[\phi]$ with some arbitrary set of weighting functions, W_j, which yields:

$$\chi = \int_R L[\phi] W_j dz \tag{24}$$

where R = a domain of interest.

If ϕ is approximated by some polynomial:

$$\tilde{\phi} = \sum_{i=1}^{n} \phi_i W_i \tag{25}$$

where W_i = approximating functions then the quantity $L[\tilde{\phi}]$ represents the residual error. For the Galerkin weighted residual method, the approximating function W_i is chosen to be the same as the weighting function W_j. The integral term becomes an error distribution principle by which the nodal values ϕ_i can be determined so that the residual error over the domain R is orthogonal to the polynomical selected for weight and interpolation functions.

By expanding the equation and integrating by parts, the reduced functional results:

$$\chi = \int_R W_j \frac{\partial \phi}{\partial t} + W_j \left[\frac{\partial}{\partial z}(v\phi) + \frac{\partial W_j}{\partial z} \varepsilon \frac{\partial \phi}{z \partial z} + W_j \alpha \phi - W_j \beta \right] dz - W_j \varepsilon \frac{\partial \phi}{z \partial z} \Big|_o^h = 0 \tag{26}$$

$$j = 1, 2 \ldots n + 1$$

Note that Equation 26 was derived by assuming no net flux across the boundary. In cases where the boundary has positive or negative net flux across it, this flux was incorporated as a source or sink term in the governing equation.

The above integral can be partitioned so that:

$$\chi = \chi_e 1 + \chi_e 2 + \chi_e 3 + \ldots + \chi_e n = \sum_{i=1}^{n} \chi_e i \tag{27}$$

where

n = the number of subdomains. This may be expanded to give:

$$\chi = \int_{z_1}^{z_2} [\ ]\, dz + \int_{z_2}^{z_3} [\ ]\, dz + \ldots + \int_{z_n}^{z_{n+1}} [\ ]\, dz \tag{28}$$

The contents in brackets in Equation 28 are the same as those in Equation 26. Equation 28 will yield a set of n+1 ordinary differential equations in terms of the ϕ_{n+1}.

Finite-Element Equations

The contributions from any typical subregion or finite element can be developed by substituting a particular polynomial approximation for ϕ into Equation 26. For simplicity, a linear approximation was chosen: i.e.,

$$\phi \simeq \tilde{\phi} = \frac{Z_{i+1} - Z}{\Delta z}\,\phi_i + \frac{Z - Z_i}{\Delta z}\,\phi_{i+1} \tag{29}$$

where $\Delta z = z_{i+1} - z_i$

In vector notation, one has:

$$\tilde{\phi}(z,t) = W_i, W_{i+1} \begin{Bmatrix} \tilde{\phi} i \\ \phi i+1 \end{Bmatrix} \tag{30}$$

where weighting functions are given by:

$$W_i = \frac{1}{\Delta z}\,(z_{i+1} - z) \tag{31}$$

$$W_{i+1} = \frac{1}{\Delta z}\,(z - z_i) \tag{32}$$

The individual terms in the functional are approximated by:

$$\frac{\partial}{\partial t} = W_1, W_2 \begin{Bmatrix} \dfrac{\partial \phi_i}{\partial z} \\ \dfrac{\partial \phi_{i+1}}{\partial z} \end{Bmatrix} \tag{33}$$

$$\frac{\partial \phi}{\partial z} = \frac{\partial W_i}{\partial z}, \frac{\partial W_{i+1}}{\partial z} \begin{matrix} \tilde{\phi} i \\ \tilde{\phi} i+1 \end{matrix} = - \left[- \frac{1}{\Delta z}, \frac{1}{\Delta z} \right] \begin{Bmatrix} \phi_i \\ \phi_{i+1} \end{Bmatrix} \tag{34}$$

Substituting these quantities into Equation 26 for a typical subdomain, a set of algebraic equations is obtained.

The results for individual terms are given below.

1. Time Dependent Term:

$$\int_{R_{ei}} W_j \frac{\partial \phi}{\partial t}\,dz = \int_{z_i}^{z_{i+1}} W_i W_j dz \left\{ \partial \phi \quad dz = \frac{\Delta z}{6} \begin{bmatrix} 2 & 1 \\ 1 & 2 \end{bmatrix} \begin{Bmatrix} \dfrac{d\phi_i}{dt} \\ \dfrac{d\phi_{i+1}}{dt} \end{Bmatrix} \right. \tag{35}$$

2. Advective Term:

$$\int_{R_{ei}} W_j \frac{\partial v \phi}{\partial z}\,dz = \int_{R_{ei}} W_j \frac{\partial v}{\partial z} \phi\, d_z + \int_{R_{ei}} W_j\, v \frac{\partial \phi}{\partial z}\, d_z =$$

$$= \begin{bmatrix} -\frac{2}{3}v_i + \frac{1}{6}v_{i+1} & \frac{1}{6}v_i + \frac{1}{3}v_{i+1} \\ -\frac{1}{3}v_i - \frac{1}{6}v_{i+1} & -\frac{1}{6}v_i + \frac{2}{3}v_{i+1} \end{bmatrix} \begin{Bmatrix} \phi_i \\ \phi_{i+1} \end{Bmatrix} \tag{36}$$

3. Diffusion Term:

$$\int_{R_{ei}} \frac{\partial W_j}{\partial z} \varepsilon_z \frac{\partial \phi}{\partial z} dz = \frac{\varepsilon_z}{\Delta z^2} \int_{z_i}^{z_{i+1}} \begin{bmatrix} 1 & -1 \\ 1 & -1 \end{bmatrix} \begin{Bmatrix} \phi_i \\ \phi_{i+1} \end{Bmatrix} dz = \frac{\varepsilon_z}{\Delta z} \begin{bmatrix} 1 & -1 \\ 1 & -1 \end{bmatrix} \begin{Bmatrix} i \\ \phi_{i+1} \end{Bmatrix} \tag{37}$$

4. Decay Term:

$$\int_{R_{ei}} W_j \alpha \phi_i dz = \alpha \int_{z_i}^{z_{i+1}} W_j W_i dz \phi_i = \frac{\alpha \Delta z}{6} \begin{bmatrix} 2 & 1 \\ 1 & 2 \end{bmatrix} \begin{Bmatrix} \phi_i \\ \phi_{i+1} \end{Bmatrix} \tag{38}$$

5. Sink/source Term:

$$\int_{R_{ei}} W_j \beta dz \; \beta \int_{z_i}^{z_{i+1}} W_j dz = \beta \Delta z \begin{Bmatrix} 1/2 \\ 1/2 \end{Bmatrix} \tag{39}$$

Where β is assumed independent of z. However, many sink/source terms in Equations 1, 9, and 21 are not independent of z and these terms are integrated according to their dependency of z. Summing up and gathering terms, one can write the element contributions to the matrix equation as finite element:

$$\sum_{j=1}^{n} \left[[P]_{ej} \begin{Bmatrix} \dot{\phi}_i \\ \dot{\phi}_{i+1} \end{Bmatrix} + [S]_{ej} \begin{Bmatrix} \phi_i \\ \phi_{i+1} \end{Bmatrix} \right] = \sum_{j=1}^{n} \{R\}_{ej} \tag{40}$$

where

$$[P]_{ej} = \Delta z \begin{bmatrix} 1/3 & 1/6 \\ 1/6 & 1/3 \end{bmatrix} \tag{41}$$

$$\{R\}_{ej} = \frac{\beta \Delta z}{2} \begin{Bmatrix} 1 \\ 1 \end{Bmatrix} \tag{42}$$

$$[S]_{ej} = \begin{matrix} (D - \frac{2}{3}V_i + \frac{1}{6}V_{i+1} + \frac{\alpha\Delta z}{3} - (D - \frac{1}{6}V_i - \frac{1}{3}V_{i+1} - \frac{\alpha\Delta z}{6} \\ -(D + \frac{1}{3}V_i + \frac{1}{6}V_{i+1} + \frac{\alpha\Delta z}{6} (D - \frac{1}{6}V_i + \frac{2}{3}V_{i+1} + \frac{\alpha\Delta z}{3} \end{matrix} \quad (43)$$

$$D = \frac{\varepsilon_z}{\Delta z}, \quad (44)$$

The summation given in Equation 27 gives the rules for construction the matrices for all finite elements; the matrices [P] and [S] become tridiagonal matrices. The final set of equations is a generalization of Equation 40.

Time-Dependent Solution

The final set of equations derived above can be expressed by:

$$[\tilde{P}] \left\{\frac{d\phi}{dt}\right\} + [\tilde{S}] \{\phi\} = \{\tilde{R}\} \quad (45)$$

where

$[\tilde{P}]$ matrix = a symmetric tridiagonal
$[\tilde{S}]$ matrix = an unsymmetric tridiagonal
$\{\tilde{R}\}$ = a load vector.

This final system of equations is approximated by a Crank-Nicholson scheme (Varga 1965):

$$[\tilde{P}] \frac{\{\phi\}^{n+1} - \{\phi\}^n}{\Delta t} = -\frac{1}{2} [\tilde{S}] \left(\{\phi\}^{n+1} + \{\phi\}^n\right) + \frac{1}{2}\left(\{R\}^{n+1} + \{R\}^n\right) \quad (46)$$

Solving the for n+I volue of , this expression can be rearranged to obtain:

$$[\bar{P}] \{\phi\}^{n+1} = [\bar{S}] \{\phi\}^n + \{\bar{R}\} \quad (47)$$

where the new coefficient matrices are:

$$[\bar{P}] = [\tilde{P}] + \left(\frac{\Delta t}{2}\right) [\tilde{S}] \quad (48)$$

$$[\bar{S}] = [\tilde{P}] - \left(\frac{\Delta t}{2}\right)[\tilde{S}] \quad (49)$$

$$\{\bar{R}\} = \Delta t \{\tilde{R}\} = \frac{\Delta t}{2} (\{R\}^{n+1} + \{R\}^n) \quad (50)$$

This type of approximation is second order correct, unconditionally stable and easily solved by most available tridiagonal solution schemes.

A computer program has been written in the FORTRAN preprocessor language FLECS to implement the model (Onishi and Wise 1979c). However, a standard FORTRAN IV version of SERATRA is also available.

3.5 LISTS OF INPUT DATA AND SIMULATION OUTPUT

SERATRA, consisting of the three submodels, is applicable to nontidal rivers and impoundments. One of the advantages of SERATRA is that it can be applied to water bodies over large longitudinal distances and shallow depths. Input data requirements for SERATRA are:

- Common Data Requirements for all the Submodels:
  - Channel geometry
  - Discharges and flow depth of the rivers during the simulation period
  - Discharges of tributaries, overland runoff and other point and nonpoint sources
  - Vertical dispersion coefficient
- Additional Requirements for Sediment Transport Submodel
  - Sediment size fraction
  - Sediment density and fall velocities for sand, silt, and clay
  - Critical shear stresses for erosion and deposition of cohesive sediment (silt and clay)
  - Erodibility coefficient of cohesive sediment

  Initial Conditions
  - Sediment concentration for each sediment size fraction
  - Bottom sediment size fraction

  Boundary Conditions
  - Sediment concentration at the upstream end of the study reach
  - Contributions of sediments from overland, tributaries and other point and nonpoint sources.

- Additional Requirements for Dissolved and Particulate Contaminant Transport Submodels:

  - Distribution coefficients and transfer rates of contaminant with sediment in each sediment size fraction (i.e., sand, silt, and clay). If values of distribution coefficients are not available, it is necessary to know clay mineral and organic sediment content to estimate these values.

  - Degradation and decay rates of contaminants

  Initial Conditions

  - Dissolved contaminant concentration

  - Particulate contaminant concentration for each sediment size fraction (i.e., those attached to sand, silt, and clay)

  Boundary Conditions

  - Dissolved and particulate contaminant concentrations for each sediment size fraction at the upstream end of the study reach

  - Contributions of dissolved and particulate contaminant concentrations from tributaries, overland, and other point and nonpoint sources.

With the input data described above, SERATRA simulates the following:

1. Sediment simulation for any given time

   - longitudinal and vertical distributions of total sediment (sum of suspended and bed load) concentration for each sediment size fraction

   - longitudinal and vertical distributions of sediment size fractions in the river bed

   - change in bed elevation (elevation changes due to sediment deposition and/or scour)

2. Contaminant simulation for any given time

   - longitudinal and vertical distributions of dissolved contaminant concentration

   - longitudinal and vertical distributions of contaminant concentration adsorbed by sediment for each sediment size fraction

- longitudinal and vertical distributions of contaminant concentrations in the bottom sediment within the bed for each sediment size fraction.

SECTION 4

MODEL APPLICATION RESULTS

As an integrated part of the CMRA Methodology for the overland and instream transport simulation and risk assessment of pesticides, SERATRA was applied to Four Mile and Wolf Creeks in Iowa to simulate migration of sediment and the pesticide, alachlor in these streams (Onishi et al. 1979b). The purpose of the CMRA Methodology application to Four Mile Creek watershed was to evaluate the methodology and not to perform a complete assessment of the pesticide. Alachlor is a preemergence herbicide used to control most annual grasses and certain broadleaf weeds. This pesticide is the most widely used herbicide in the predominantly agricultural Four Mile Creek watershed (Baker et al. 1979). The study area for the instream modeling was a 67.6 km reach between river kilometer 19.3 in Four Mile Creek and the mouth of the Wolf Creek, as shown in Figure 1. Four Mile Creek joins Wolf Creek at river kilometer 48.3 of Wolf Creek. Simulations of sediment and alachlor migration in these streams were performed for the three-year period between June 1971 and May 1974.

The following assumptions were made to set up the ARM model: For each of the three catchments, dates for plowing, planting and cultivating were randomly selected within the periods of April 1 - May 1, May 5 - June 1, and May 30 - July 1, respectively. Soybeans were assumed to be the major crop planted in the study area, and alachlor was applied to the soybeans the day after planting. The only constraint on the selection of a pesticide application date was that it would not occur on the same day as a storm event occurred. The application rates of alachlor for Gladbook (344 ha) and Southern (444 ha) Catchments were selected to be 0.8 kg/ha, while the application rate for Northern Catchment (660 ha) was assumed to be 2.3 kg/ha. Detailed description of the ARM simulation was presented in Onishi et al. (1979). Computed sediment and pesticide loads by the ARM model were, in turn, supplied to SERATRA as input data. The computed runoff was used as input to EXPLORE-I (Baca et al. 1973; Onishi 1979b). Since SERATRA requires depth and velocity distributions in Four Mile and Wolf Creeks as input data, we applied a hydrodynamic submodel of the general water quality model EXPLORE-I to Four Mile and Wolf Creeks to predict depth and velocity distributions for the simulation period. Runoff from the three catchments within the Four Mile Creek watershed was assumed to reach Four Mile Creek at river kilometer 9.7 (see Figure 1).

Very few measured data were available for the instream pesticide modeling. Discharge measurements of Four Mile Creek conducted at Traer (river kilometer 4.22) during the three year simulation period indicate

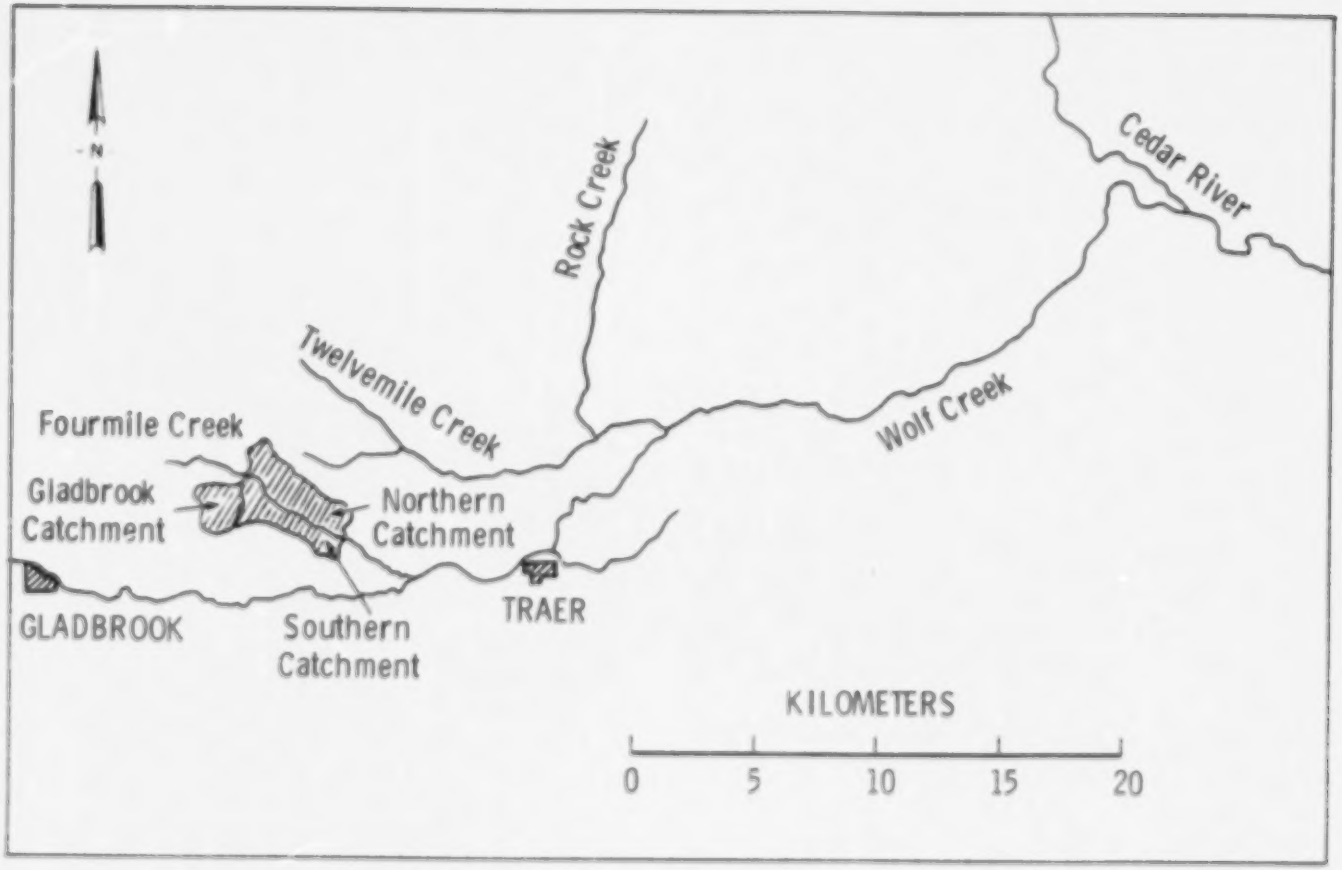

Figure 1. Four Mile and Wolf Creek in Iowa.

the large variation of daily discharge, ranging from 9.65 m^3/sec to 0.006 m^3/sec. An average discharge at Traer during this period was 0.46 m^3/sec. Because the purpose of the methodology application to Four Mile and Wolf Creeks was to evaluate the methodology and not to perform an assessment in this area, some simplification of flow data was performed.

The base flow of Four Mile Creek without runoff contributions was assumed to be 2 m^3/sec. Detailed test conditions for sediment and pesticide transport modeling are shown in Table 1. Based on field data obtained by Iowa State University (Baker et al. 1979), it was assumed that the river sediment consists of 65% sand, 15% silt and 20% clay. For eroded soil from the overland, Baker et al. (1979) show the variation in a particle size distribution as a function of time and sediment concentration. Based on these particle size distribution analyses performed by the Iowa State University on selected runoff samples, calculated total sediment loading from these three catchments were assumed to consist of 0% sand, 40% silt and 60% clay. Particle sizes of sand, silt and clay were assumed to be 0.350 mm, 0.016 mm, and 0.0014 mm, respectively. No field or laboratory studies were performed to evaluate critical shear stresses (τ_{cRj} and τ_{cDj}) and the erodibility coefficient (M_j), needed to calculate erosion and deposition of cohesive sediments. These parameters were determined through a trial and error calibration precedure. The bed shear stresses at each location for each time step were calculated by SERATRA code internally with a known hydraulic condition.

The distribution coefficient of alachlor associated with the bulk sediment was estimated to be 50 ml/g in the receiving streams (Baker et al. 1979). In this application, adsorption/desorption processes were assumed to be completely reversible processes. In this study, distribution coefficients for both adsorption and desorption, Kd and Kd values of alachlor with sand, silt and clay were rather arbitrary assumed to be 2, 20, and 100 ml/g. The total pesticide alachlor for each storm event was then distributed to each sediment size fraction as follows: A ratio of the selected Kd and Kd values of sand to those of silt and clay is 1:10:50. Hence for a equal amount of sand, silt and clay, clay contains five times more alachlor than silt, which in turn contains 10 times more alachlor than sand. Since the sediment loading from overland was assumed to be 40% silt and 60% clay, total particulate alachlor contributed from the three catchments was divided into 0%, 12% and 88% each associated with eroded overland sand, silt and clay, respectively at the stream edge. Because of the lack of available data, the transfer rates, K_j and K_j, for alachlor to moving sediment and stationary bed sediment to reach to an equilibrium condition assigned by distribution coefficients were arbitrarily assigned to be 0.36 and 0.001 per hour, respectively. Based on the sediment size fraction ratio and the Kd and Kd values for the sediment of each size fraction, it was determined that 0%, 12% and 88% of particulate pesticide loading from overland at Four Mile Creek, as computed by ARM, were associated with sand, silt and clay, respectively. Althrough SERATRA simulates various chemical and biological degradation of dissolved pesticides individually, there were no available data to enable the simulation of degradation by

Table 1. Test conditions for sediment and pesticide transport modeling.

Base Flow, m^3/sec	
Four Mile Creek	2
Wolf Creek	7
Manning Coefficient	
Four Mile Creek	0.07
Wolf Creek	0.04
Sediment Sizes, mm	
Sand	0.35
Silt	0.016
Clay	0.0014
Bed Sediment Size Fraction, %	
Sand	65
Silt	15
Clay	20
Size Fraction of Eroded Sediment from Overland, %	
Sand	0
Silt	40
Clay	60
Erodibility Coefficient, kg/m^3	
Four Mile Creek	
Silt	1×10^{-4}
Clay	1×10^{-4}
Wolf Creek	
Silt	1×10^{-4}
Clay	1×10^{-4}
Critical Shear Stress for Erosion, kg/m^2	
Four Mile Creek	
Silt	1.5
Clay	1.7
Wolf Creek	
Silt	0.55
Clay	0.6
Critical Shear Stress for Deposition, kg/m^2	
Four Mile Creek	
Silt	0.7
Clay	0.6
Wolf Creek	
Silt	0.4
Clay	0.3
Vertical Diffusion Coefficient, m^2/sec	1×10^{-6}
Distribution Coefficient, m^3/kg	
With Sand	0.002
Silt	0.020
Clay	0.10
Transfer Rate, 1/hr	
Moving Sediment	0.36
Non-moving Sediment	0.001
Total Alachlor Degradation, 1/hr	0.003

each process. Hence in this study, all pesticide degradation was lumped into a first order reaction having a degradation rate of 0.003 per hour. This rate was estimated from preliminary information supplied by Monsanto Agricultural Product Co.

Simulation of sediment and alachlor transport was conducted for each of the following substances: 1) sand, 2) silt, 3) clay, 4) dissolved alachlor, 5) particulate alachlor associated with sand, 6) particulate alachlor attached to silt, and 7) particulate alachlor adsorbed by clay. The modeling procedure for SERATRA involved simulating sediment transport of sand, silt and clay. The results were then used to simulate dissolved and particulate alachlor by including the effects of alachlor-sediment interaction. Finally, changes in stream bed conditions were recorded, including: 1) stream bed elevation change, 2) vertical and longitudinal distributions of ratios of sand, silt and clay within the bed, and 3) vertical and longitudinal distributions of alachlor within the stream bed.

CASE 1. CALIBRATION RUN

Calibration of EXPLORE-I to obtain proper depth and velocity distributions in Four Mile and Wolf Creeks was performed using the largest predicted runoff event (using the overland model, ARM) during the three-year similation period. This event resulted in the maximum discharge of 18.1 m^3/sec in Four Mile Creek. The duration of the calibration run was 10 days starting from July 8 to July 17, 1971. After numerous trial runs, the proper Manning coefficients in Four Mile and Wolf Creeks were determined to be 0.07 and 0.04, respectively. These Manning coefficient values were judged reasonable for these small streams.

After ensuring mass conservation, EXPLORE-I and ARM simulation results were input to SERATRA for the model calibration. The only parameters and coefficients that require adjustment are the vertical dispersion coefficient and the three parameters, M_j, τ_{cRj}, and τ_{cDj}, used to calculate deposition and erosion rates of cohesive sediments (see Equations 7 and 8). Transport of noncohesive sediments (sand) does not require the model calibration. The other parameters (e.g., pesticide distribution coefficients and degradation rate, sediment sizes, etc) are determined by theoretical and experimental analyses and field conditions prior to the model simulation. Thus most of the calibration effort was oriented toward reproducing sediment distribution patterns similar to the actual or estimated longitudinal and vertical distributions of sediment concentrations for the 67.6-km study reach. For model calibration, Four Mile and Wolf Creeks were divided into fourteen 4.83-km segments. A fifteen-minute time step was used. After trial and error, the values shown in Table 1 were selected for M_j, τ_{cRj}, τ_{cDj}. The vertical dispersion coefficient was selected to be 1.0×10^{-6} m^2/sec.

Time variations of computed sediment concentration for each sediment size fraction and the sum of the three size fractions at the mouth of Four Mile Creek are shown in Figure 2. This figure indicates that the majority of sediment is clay. Figure 3 shows time variations of computed

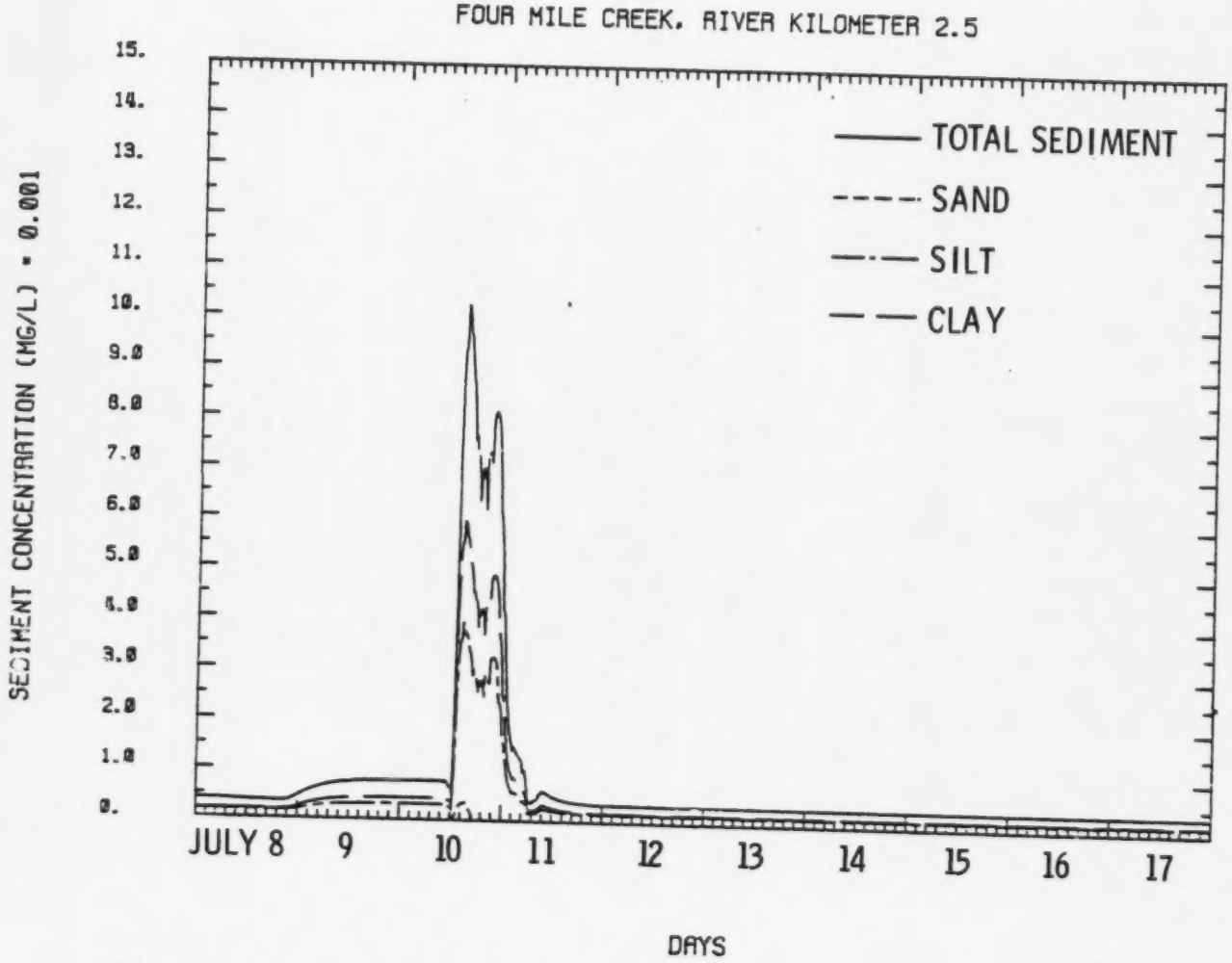

Figure 2. Time variations of simulated concentrations of sand, silt, clay and total sediment at Four Mile Creek River kilometer 2.5.

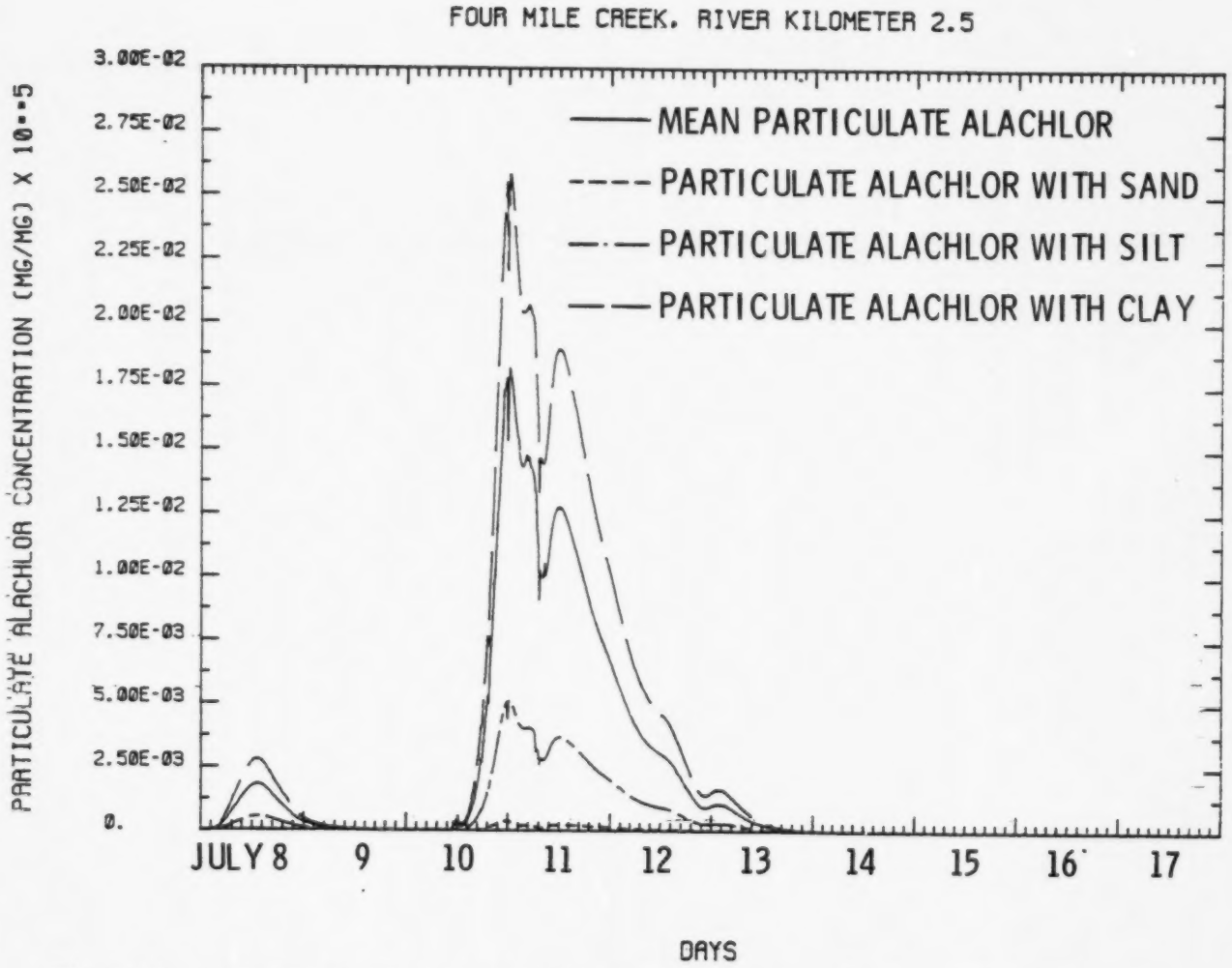

Figure 3. Time variations of simulated particulate alachlor concentrations associated with sand, silt and clay, together with mean particulate alachlor concentrations at Four Mile Creek River kilometer 2.5

particulate alachlor associated with each sediment size fraction, together with mean particulate alachlor concentrations (weighted average of three particulate alachlor concentrations associated with sand, silt and clay) at the mouth. Because clay has the largest Kd value, the particulate pesticide concentration associated with clay has the highest concentration. Sand contains the lowest pesticide concentration. Variations of computed dissolved, particulate, and total (sum of dissolved and particulate pesticide concentrations) alachlor concentrations with time at the Four Mile Creek mouth are shown in Figure 4. The figure reveals that more than 75% of alachlor near the mouth of Four Mile Creek was transported in the dissolved form and that up to 25% of alachlor was carried by sediment. This implies that sediment transport becomes important when a pesticide has a large distribution coefficient, Kd, or when a receiving water body contains very high sediment concentrations.

Vertical distributions of sediment and alachlor concentrations at Four Mile Creek River Kilometer 2.5 are shown in Figures 5, 6 and 7. In these figures, elevations of water and bed surfaces are 272.56 m and 271.77 m, respectively. Figure 5 indicates that all suspended sediments have higher concentrations near the river bed, but cohesive sediments show relatively more uniform vertical distributions. This is due to the smaller fall velocities of silt and clay as compared to the fall velocity of sand. Figure 6 presents vertical distributions of particulate alachlor concentrations per unit weight of sand, silt and clay. This figure reveals that except those attached to sand, particulate alachlor concentrations are almost vertically uniform. Vertical distributions of average particulate (weighted average of particulate alachlor associated with sand, silt and clay), dissolved and total alachlor concentrations are shown in Figure 7. In this figure, dissolved alachlor concentration is also shown to be almost vertically uniform. However, the particulate alachlor concentration per unit volume of water indicates higher concentration near the river bed due to higher sediment concentrations near the bed. The total alachlor concentration (sum of dissolved and particulate alachlor concentrations) reflects patterns of dissolved and particulate alachlor distributions. Because of the lack of field data, model calibration was not performed as rigorously as it should be.

CASE 2. THREE-YEAR SIMULATION RUN

Following model calibration, EXPLORE-I and SERATRA were used to simulate pesticide migration for the three-year duration between June 1971 and May 1974. For this case, the entire study reach was divided into seven equal-distance segments and a 30-minute time step was used to reduce the required computational time. Some of the simulation results are shown in Figures 8 through 24.

Figure 8 shows the time variation of flow rate calculated near the mouth of Wolf Creek. The figure reveals that all 10 high flows during the three-year simulation period occurred in summer and fall. Snow melt did not produce significant runoff to receiving rates during this study period. Time variation of total sediment concentrations near the Wolf Creek mouth is shown in Figure 9, which clearly indicates a small number

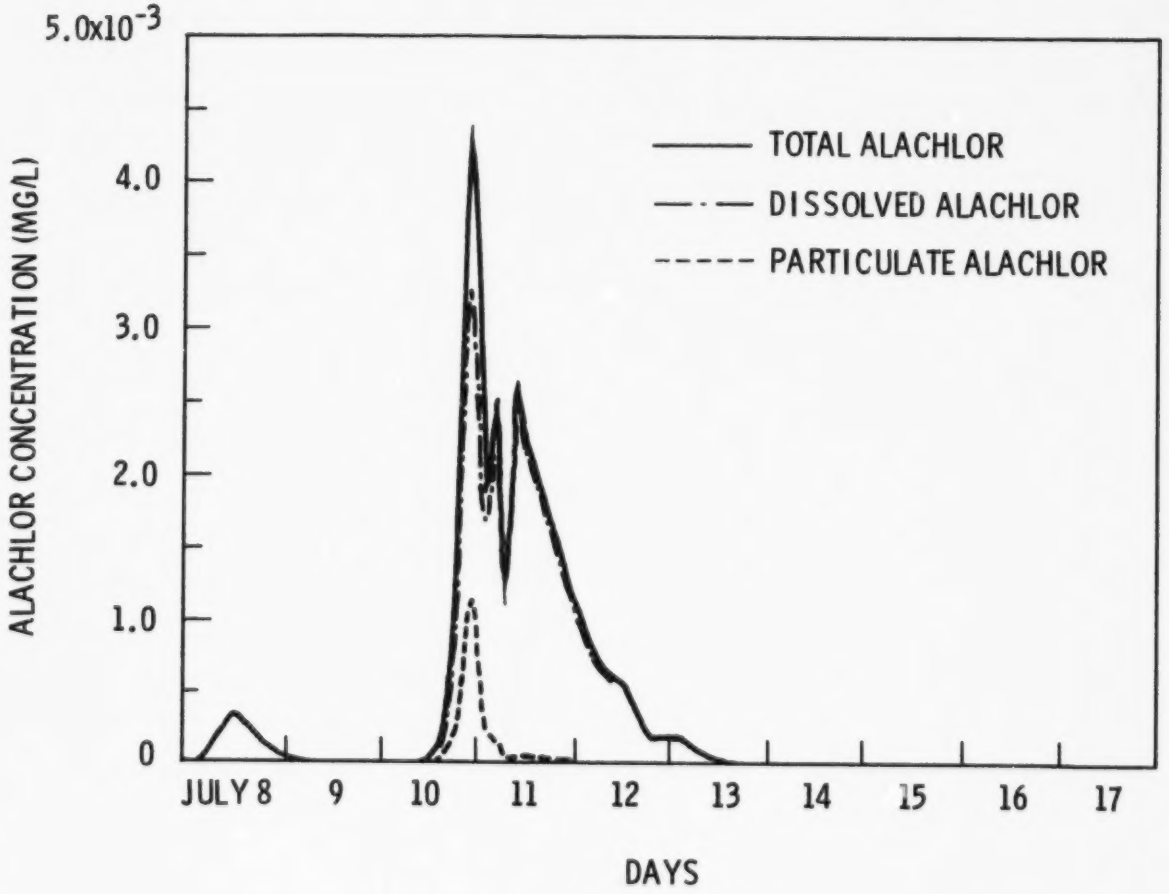

Figure 4. Time variations of simulated dissolved, particulate and total alachlor concentrations at Four Mile Creek River kilometer 2.5

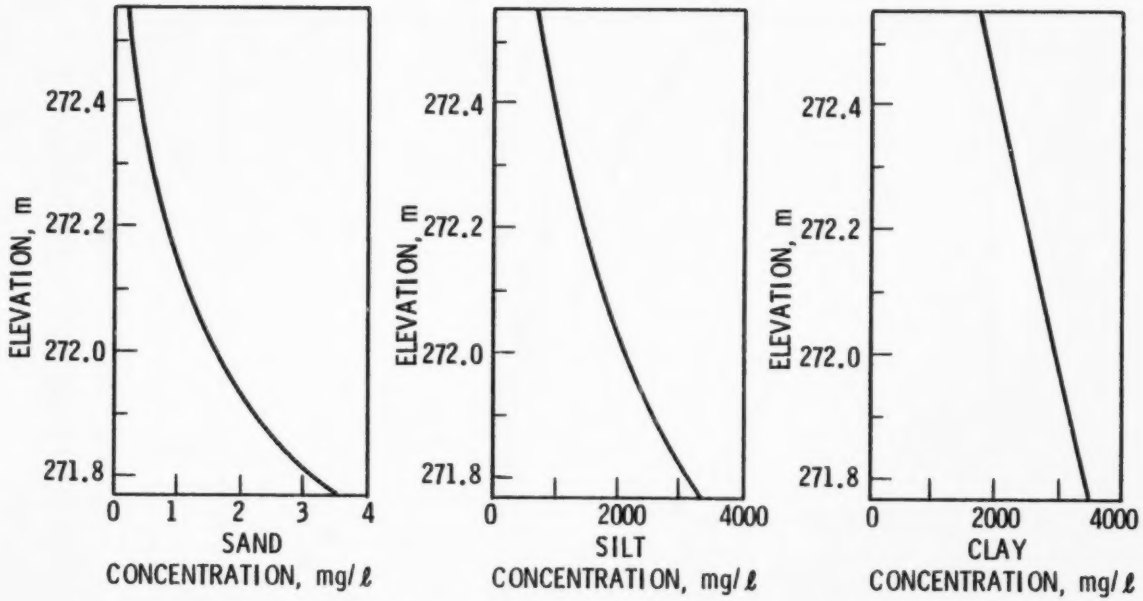

Figure 5. Vertical distribution of simulated sediment concentrations at Four Mile Creek River kilometer 2.5 at 12:00 p.m., July 10, 1971.

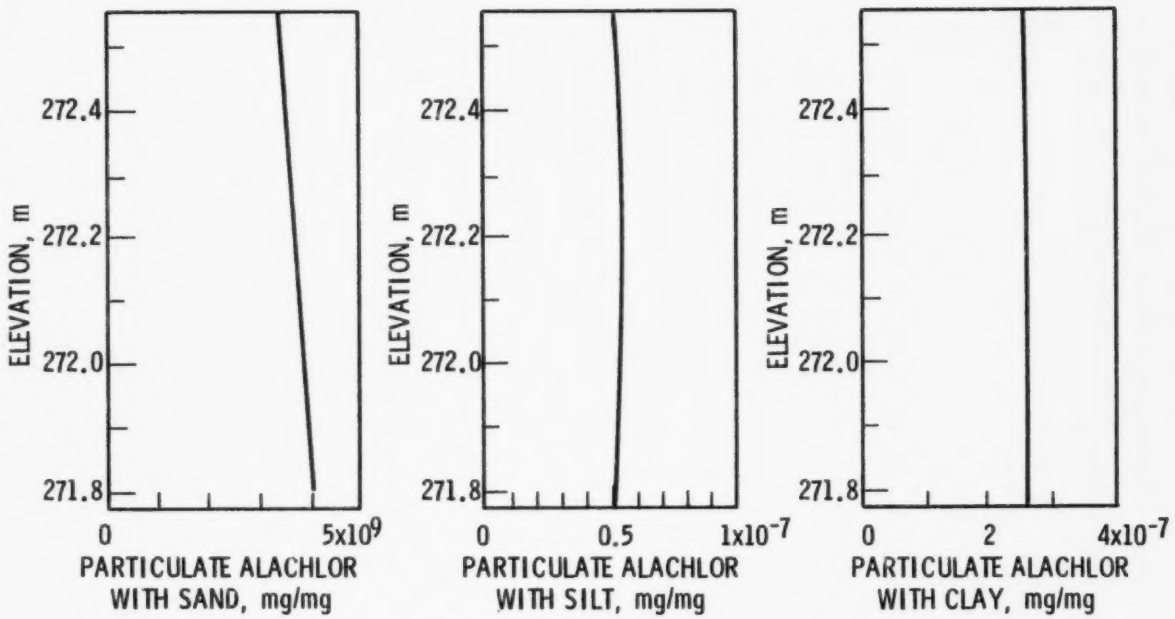

Figure 6. Vertical distributions of simulated particulate alachlor adsorbed by sediments at Four Mile Creek kilometer 2.5 at 12:00 p.m., July 10, 1971.

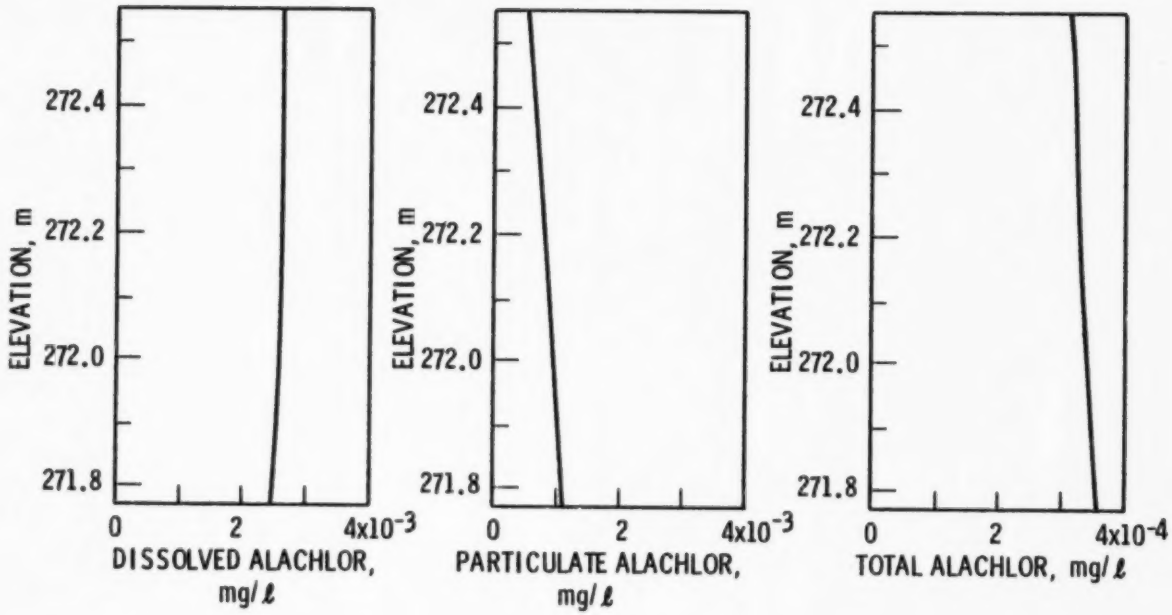

Figure 7. Vertical distributions of simulated dissolved, particulate and total alachlor concentrations at Four Mile Creek River kilometer 2.5 at 12:00 p.m., July 10, 1971.

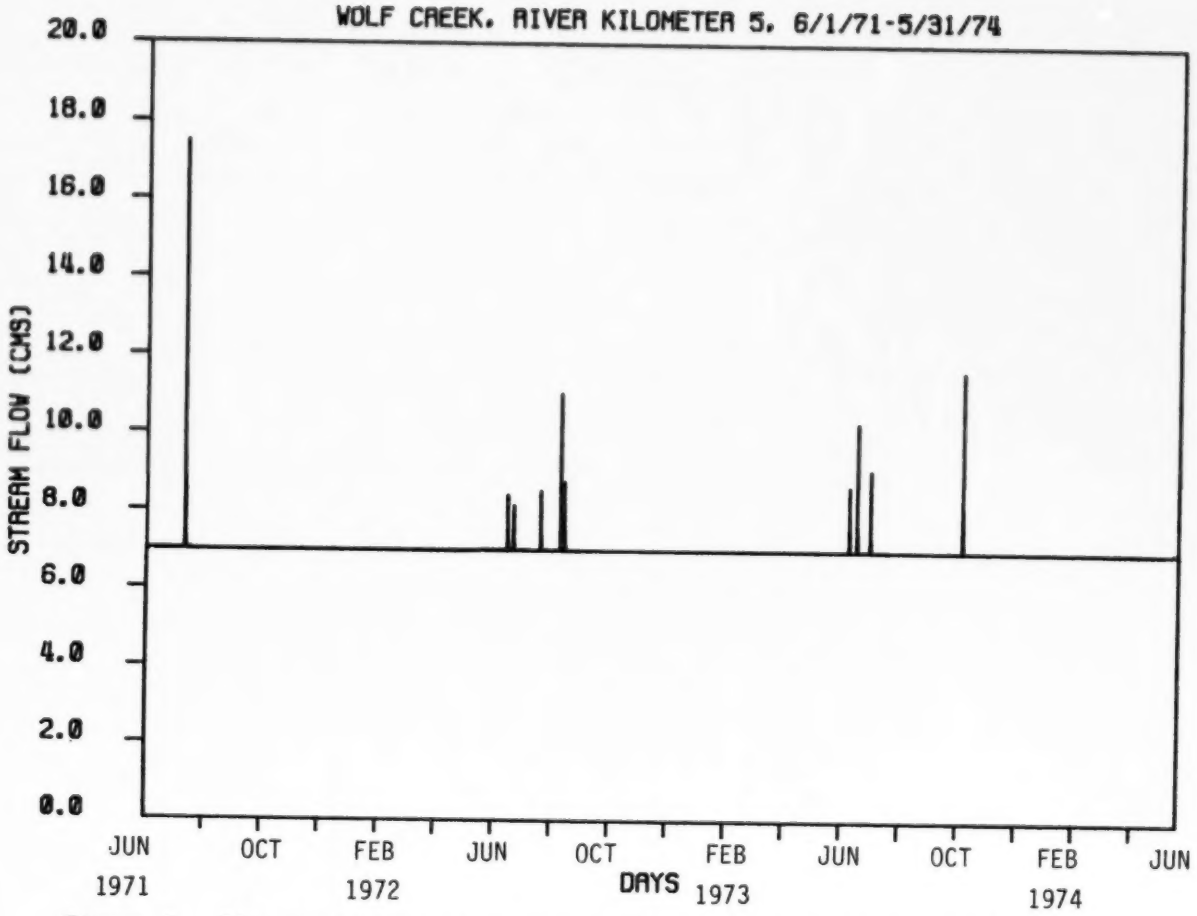

Figure 8. Time variations of predicted flow rate at Wolf Creek River kilometer 5 during the three-year simulation period.

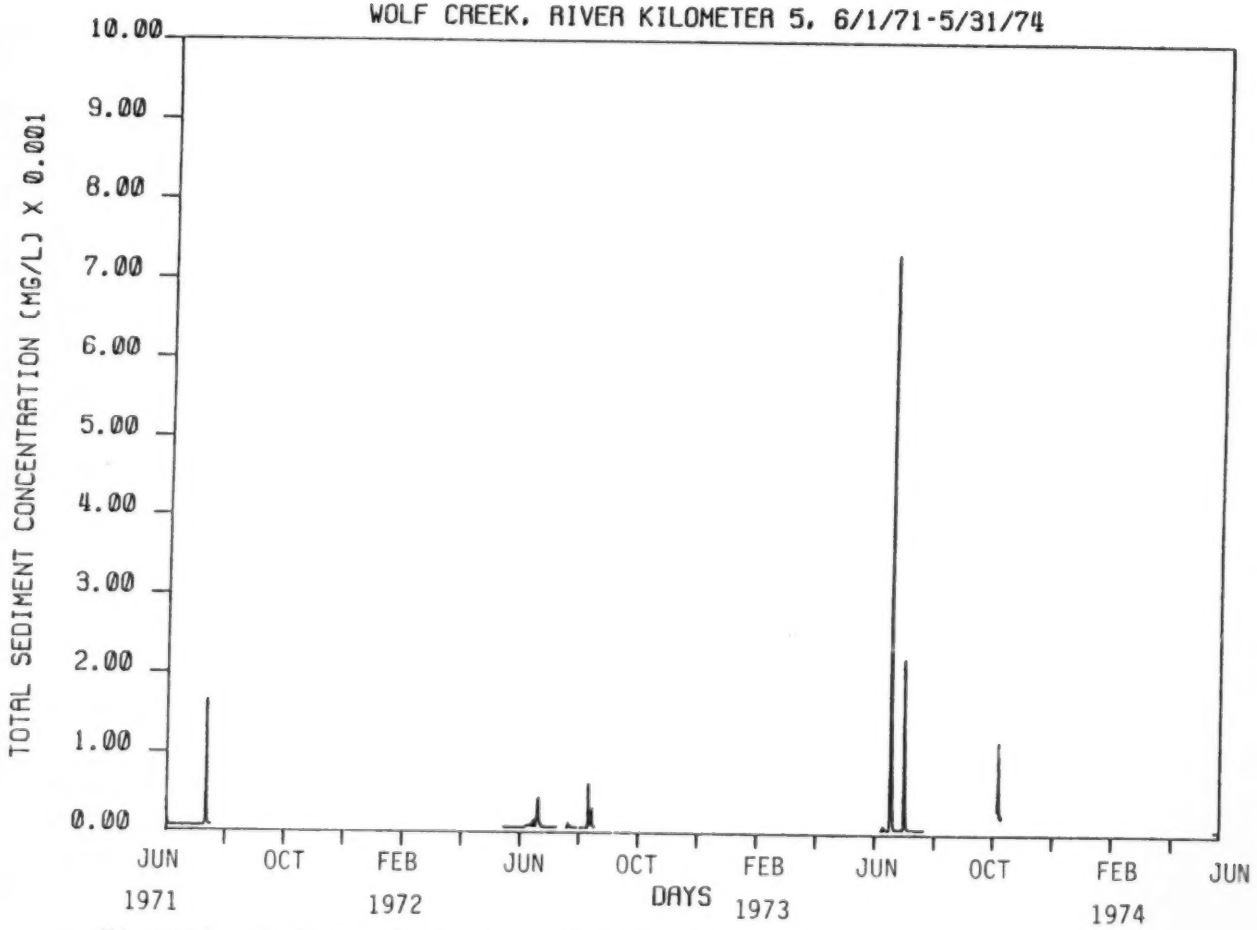

Figure 9. Time variation of predicted total sediment concentration at Wolf Creek River Kilometer 5 during the three-year simulation period.

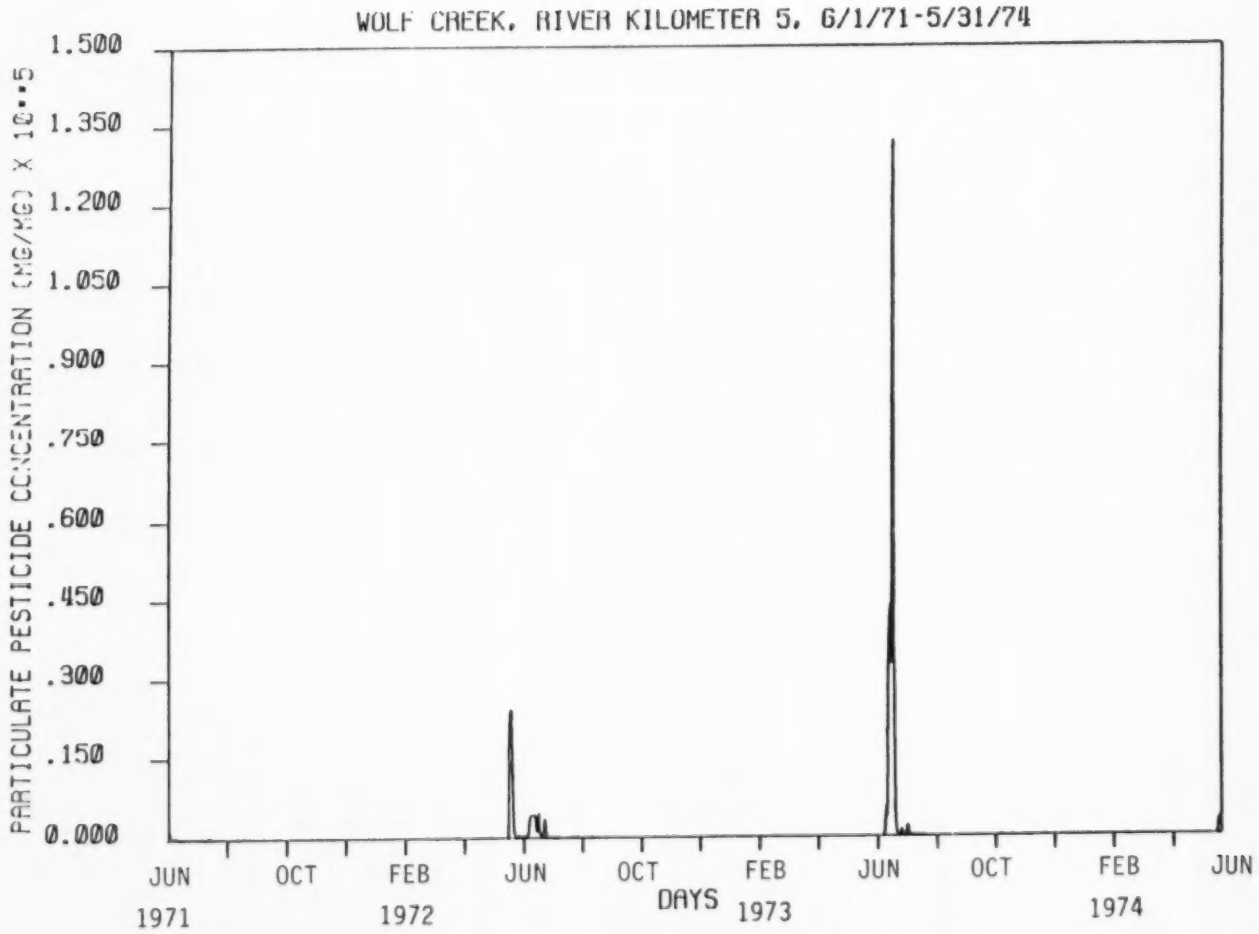

Figure 10. Time variation of predicted particulate alachlor concentration per unit weight of sediment at Wolf Creek River kilometer 5 during the three-year simulation period.

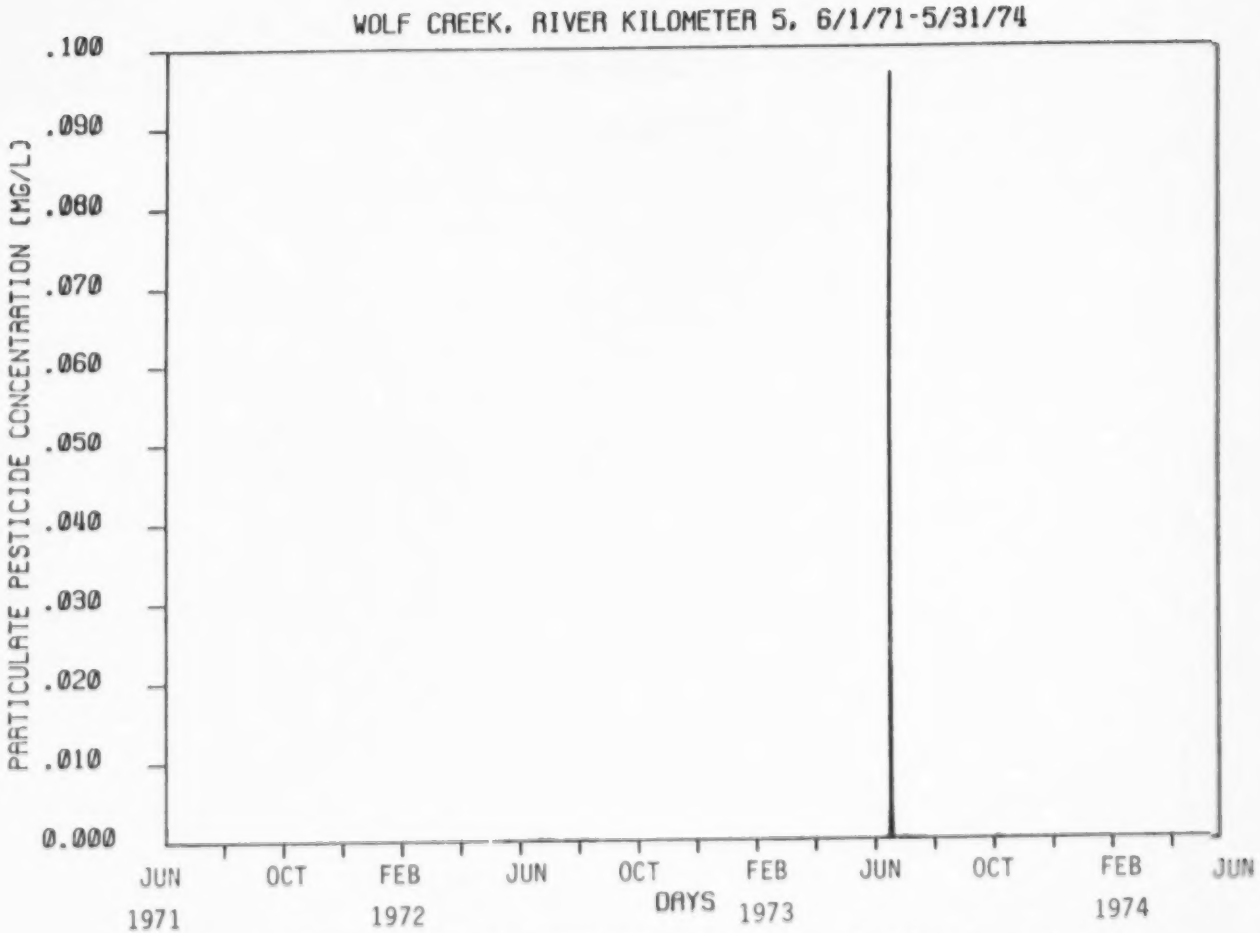

Figure 11. Time variation of predicted particulate alachlor concentration per unit volume of water at Wolf Creek River kilometer 5 during the three-year simulation period.

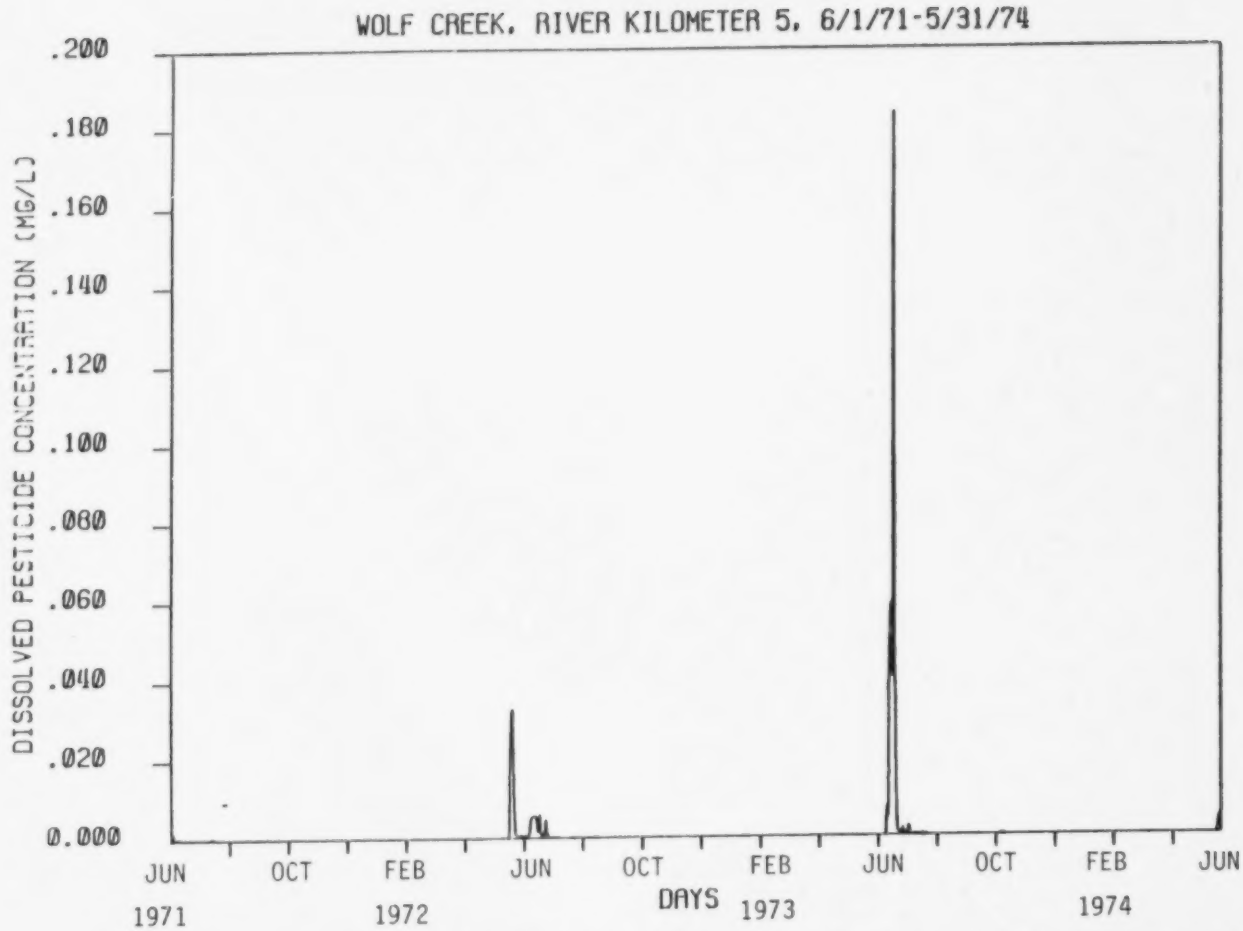

Figure 12. Time variation of predicted dissolved alachlor concentration at Wolf Creek River kilometer 5 during the three-year simulation period.

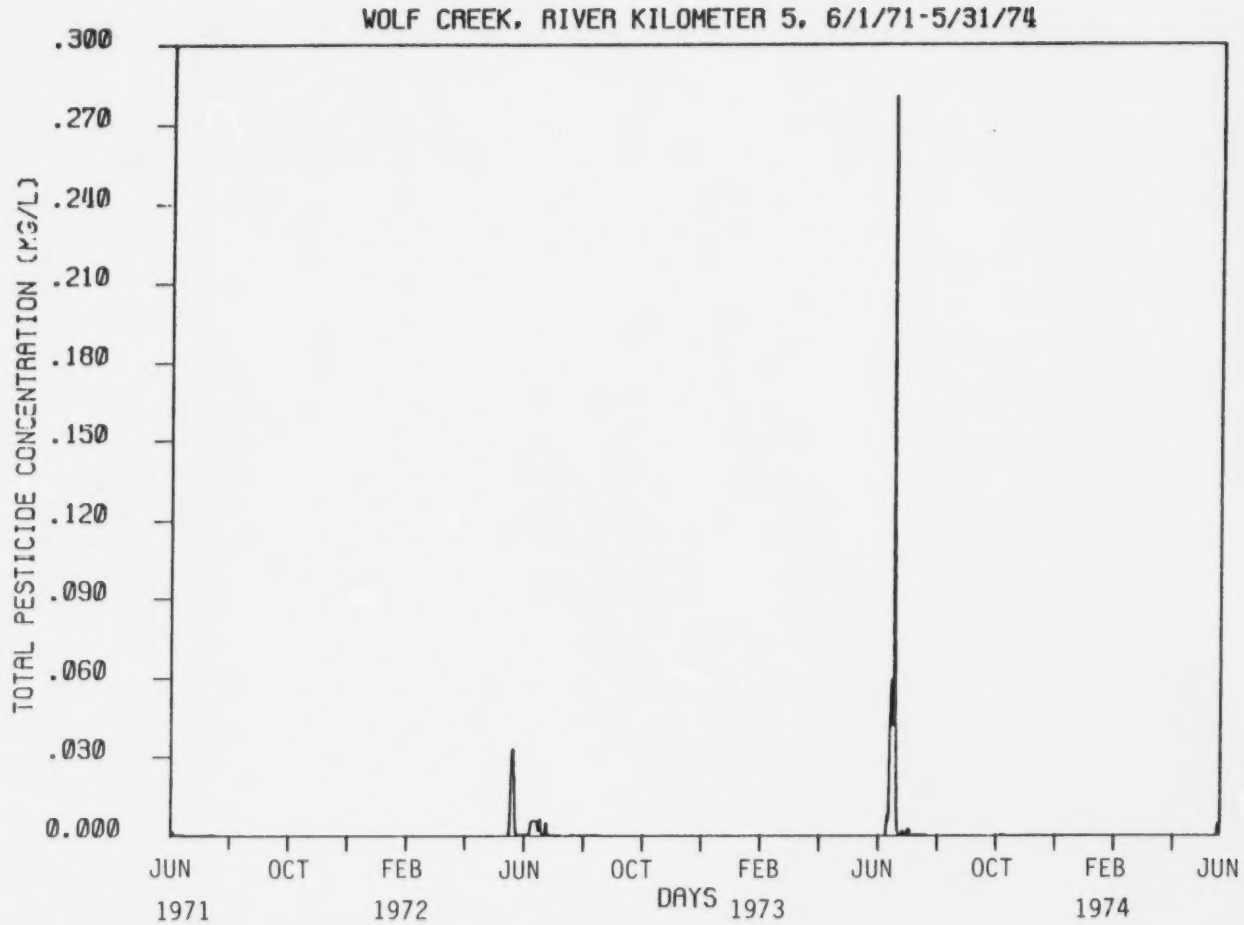

Figure 13. Time variation of predicted total alachlor concentration at Wolf Creek River kilometer 5 during the three-year simulation period.

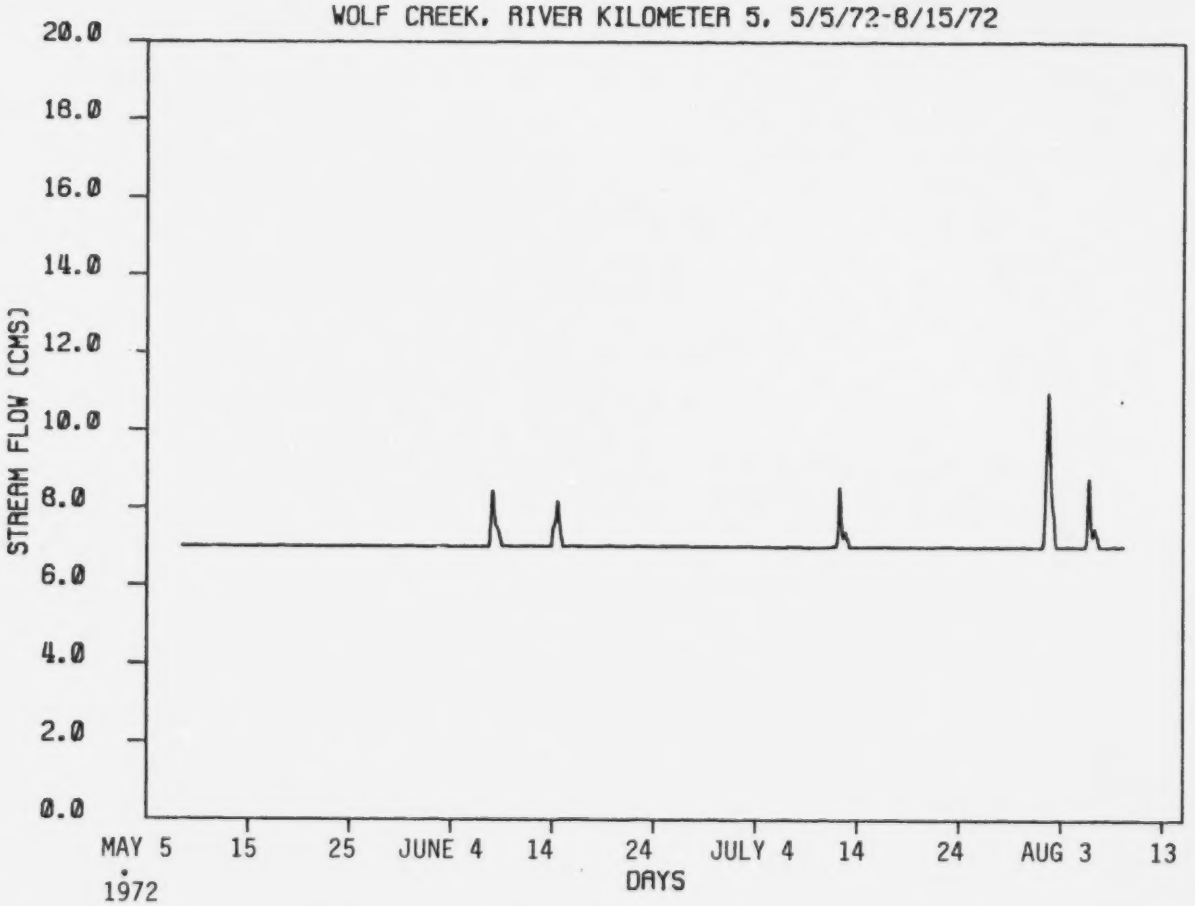

Figure 14. Time variation of simulated flow rate at Wolf Creek River kilometer 5 during May 5, 1972 to August 15, 1972.

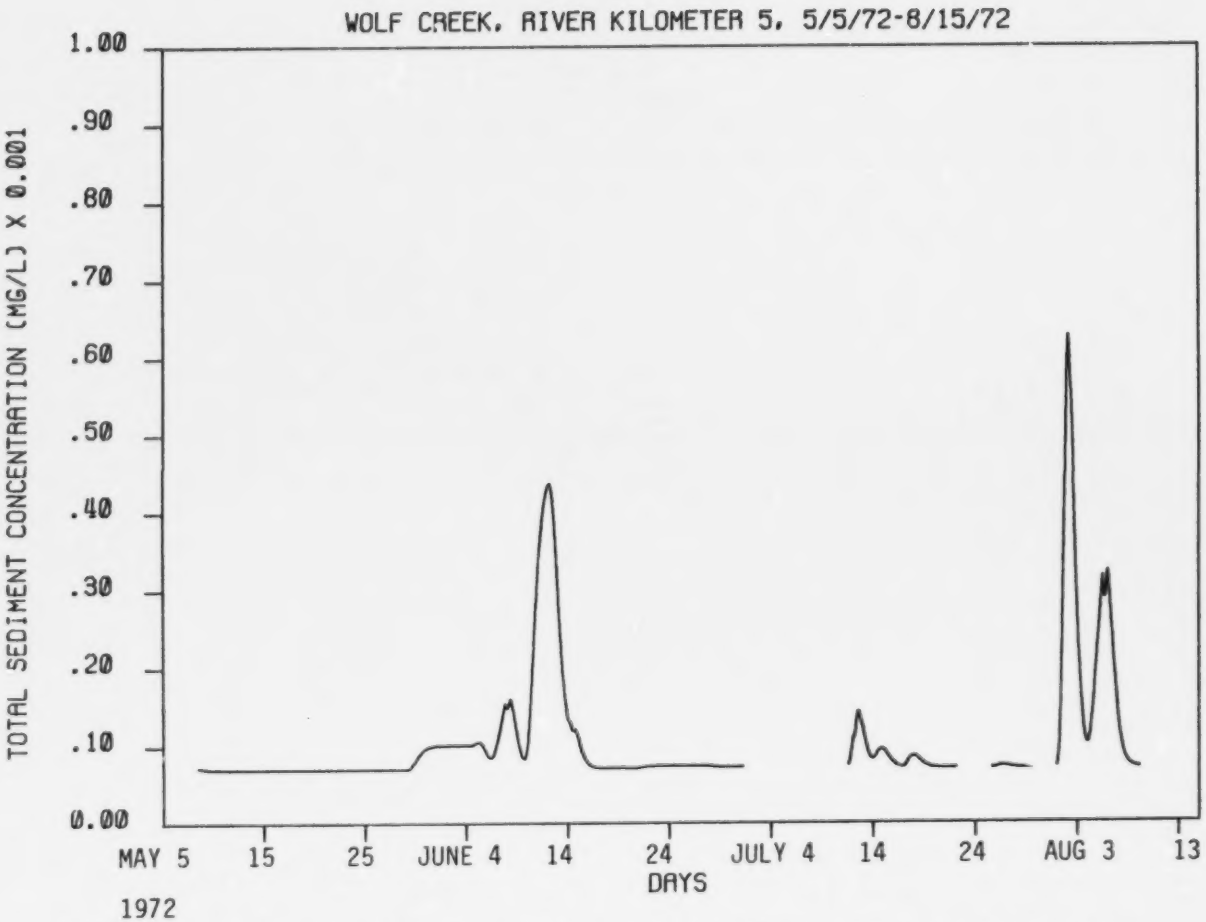

Figure 15. Time variation of simulated total sediment concentration at Wolf Creek River kilometer 5 during May 5, 1972 to August 15, 1972.

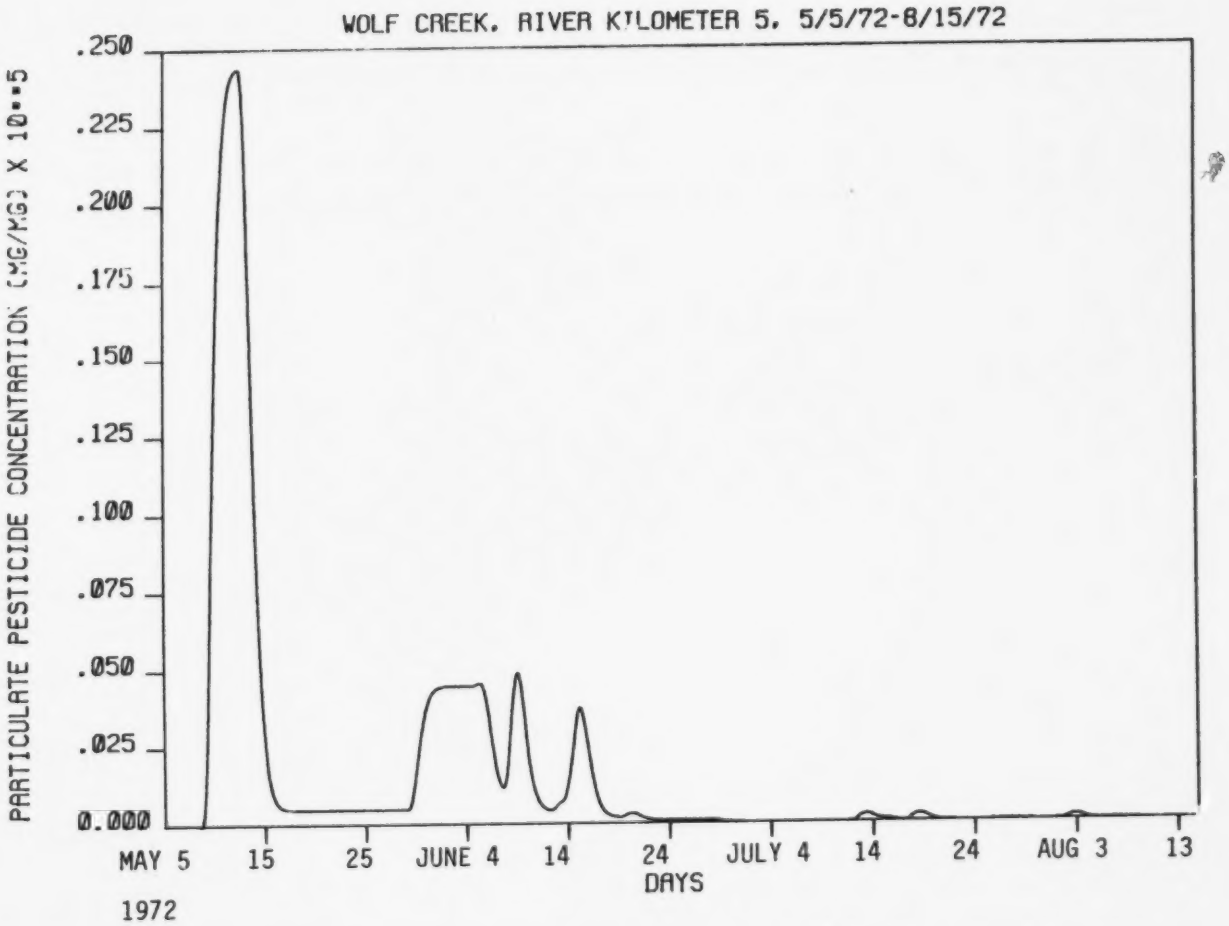

Figure 16. Time variation of simulated particulate alachlor concentration per unit weight of sediment at Wolf Creek River kilometer 5 during May 5, 1972 to August 15, 1972

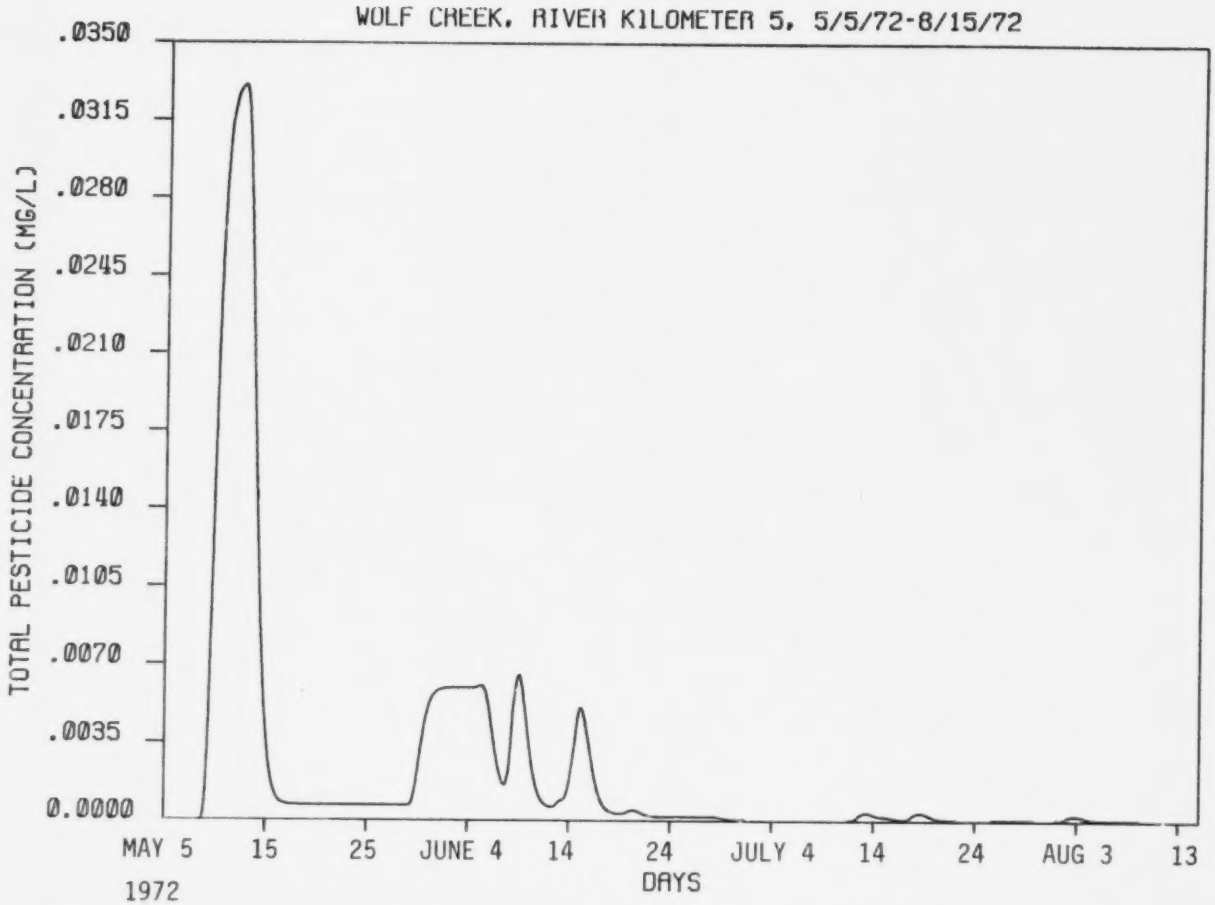

Figure 17. Time variation of simulated total alachlor concentration at Wolf Creek River kilometer 5 during May 5, 1972 to August 15, 1972.

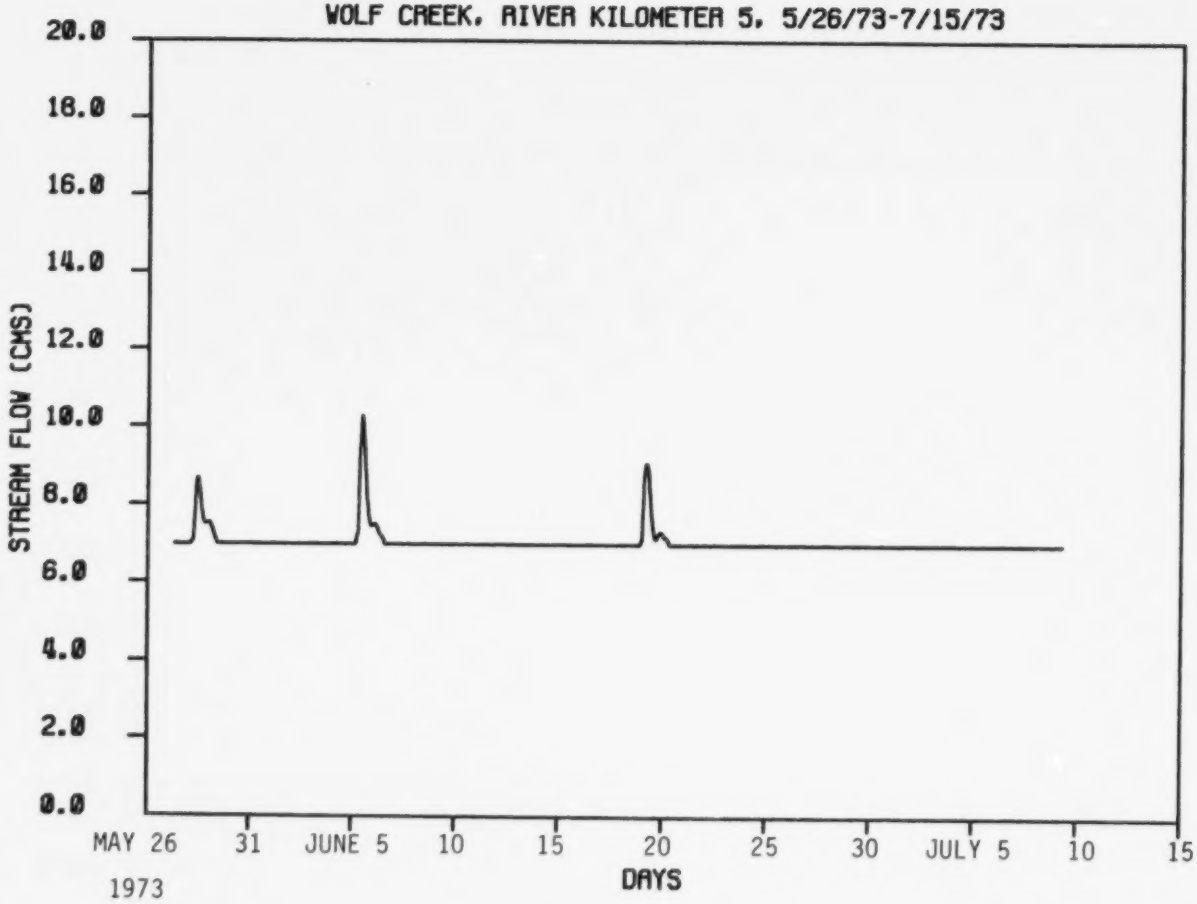

Figure 18. Time variation of simulated flow rate at Wolf Creek River kilometer 5 during May 26, 1973 to July 15, 1973.

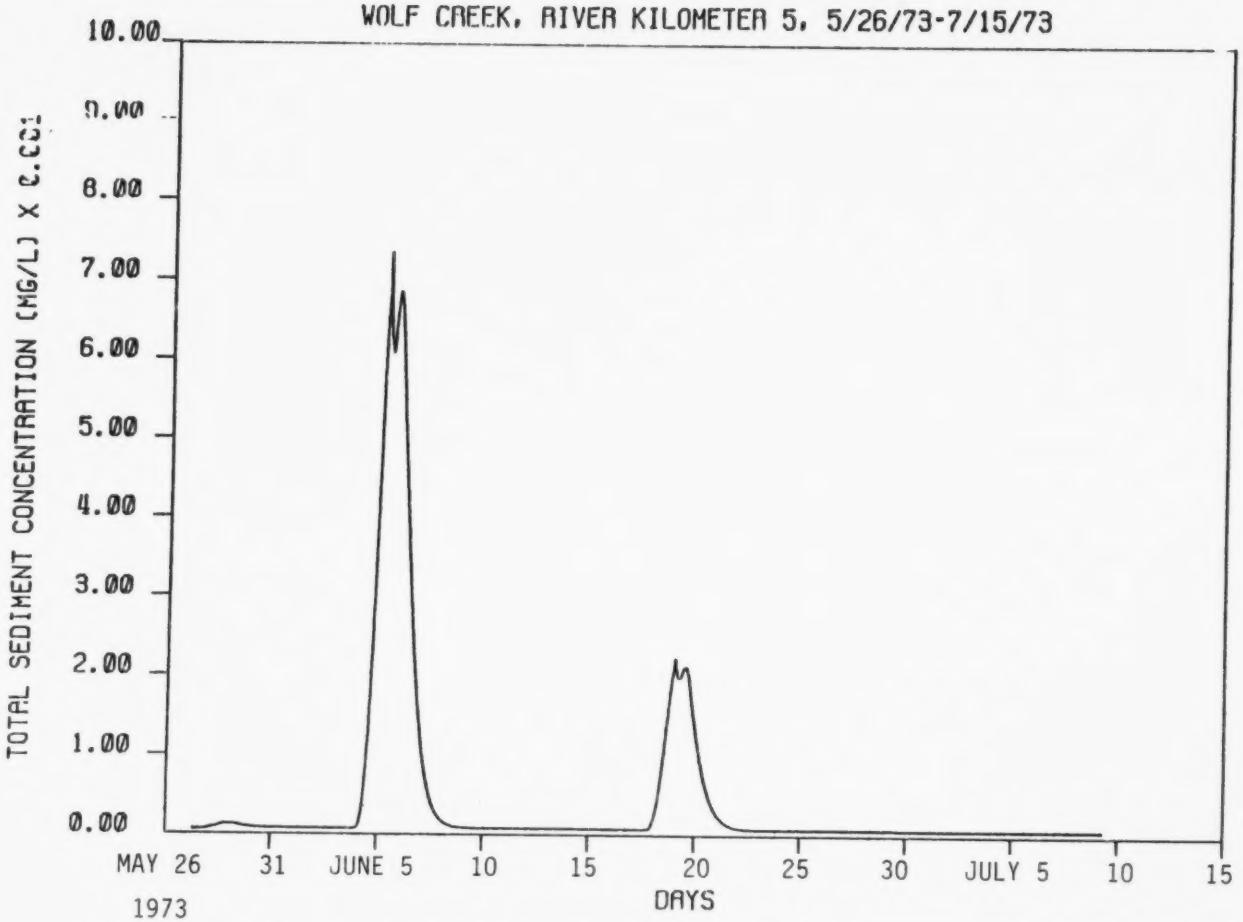

Figure 19. Time variation of simulated total sediment concentration at Wolf Creek River kilometer 5 during May 26, 1973 to July 15, 1973.

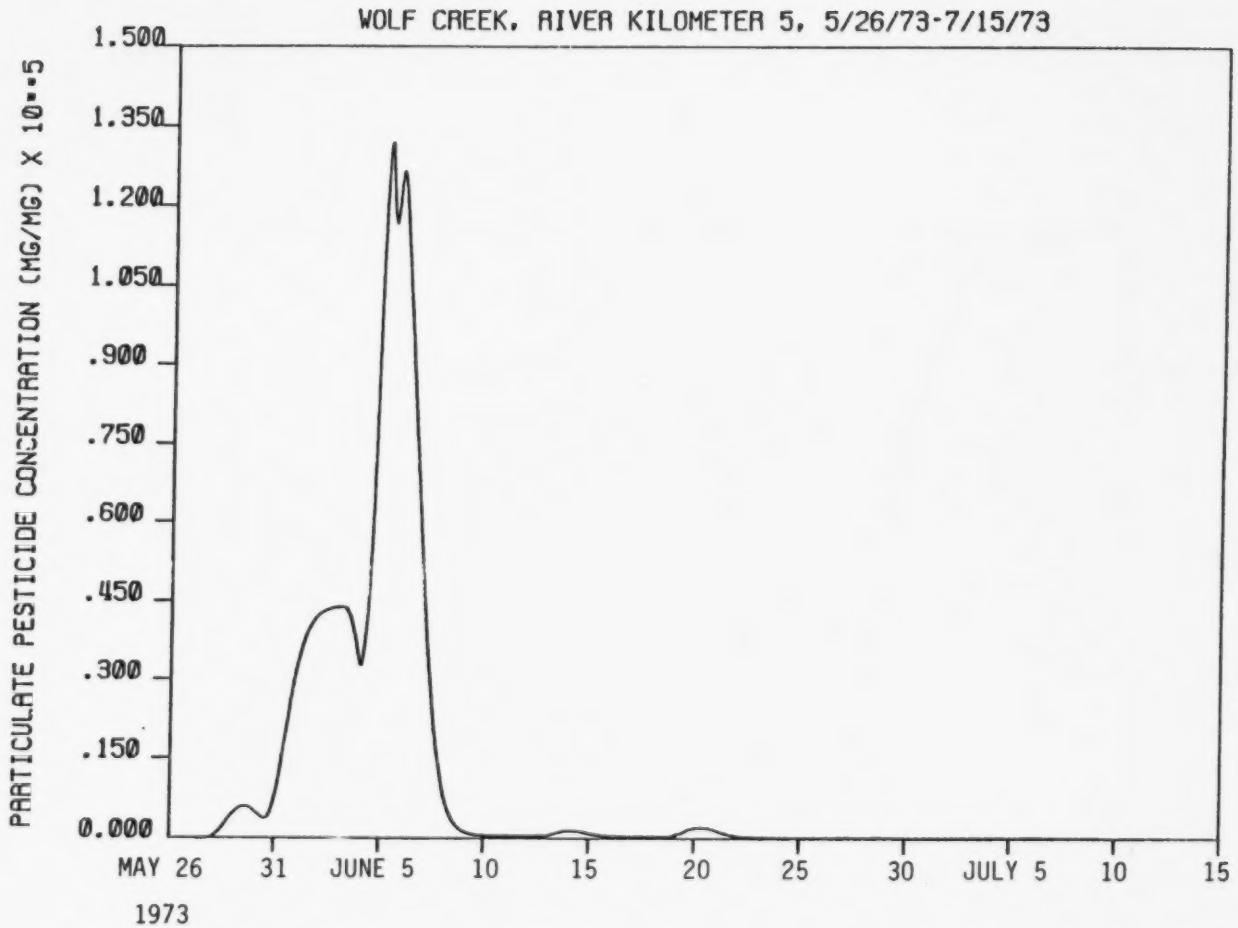

Figure 20. Time variation of simulated particulate alachlor concentration at Wolf Creek River kilometer 5 during May 26, 1973 to July 15, 1973.

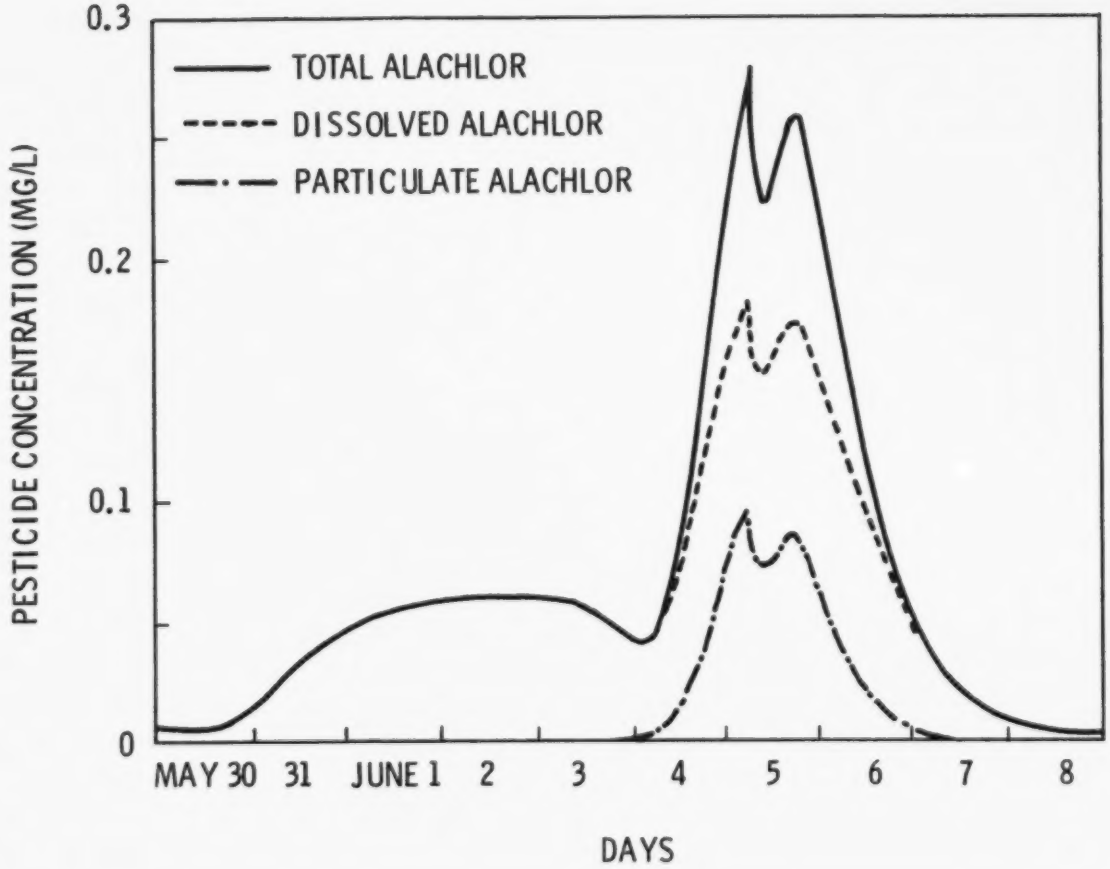

Figure 21. Time variation of simulated dissolved, particulate and total alachlor concentrations at Wolf Creek River kilometer 5 during May 30, 1973 to June 9, 1973.

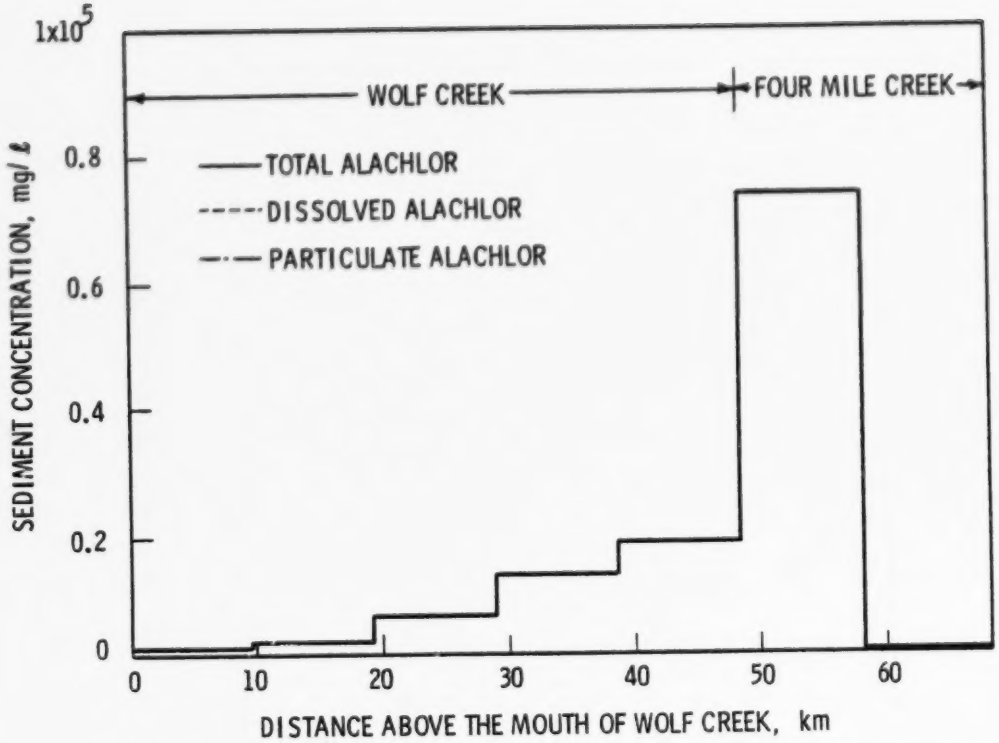

Figure 22. Longitudinal distribution of total sediment concentration at 6 a.m., July 4, 1973.

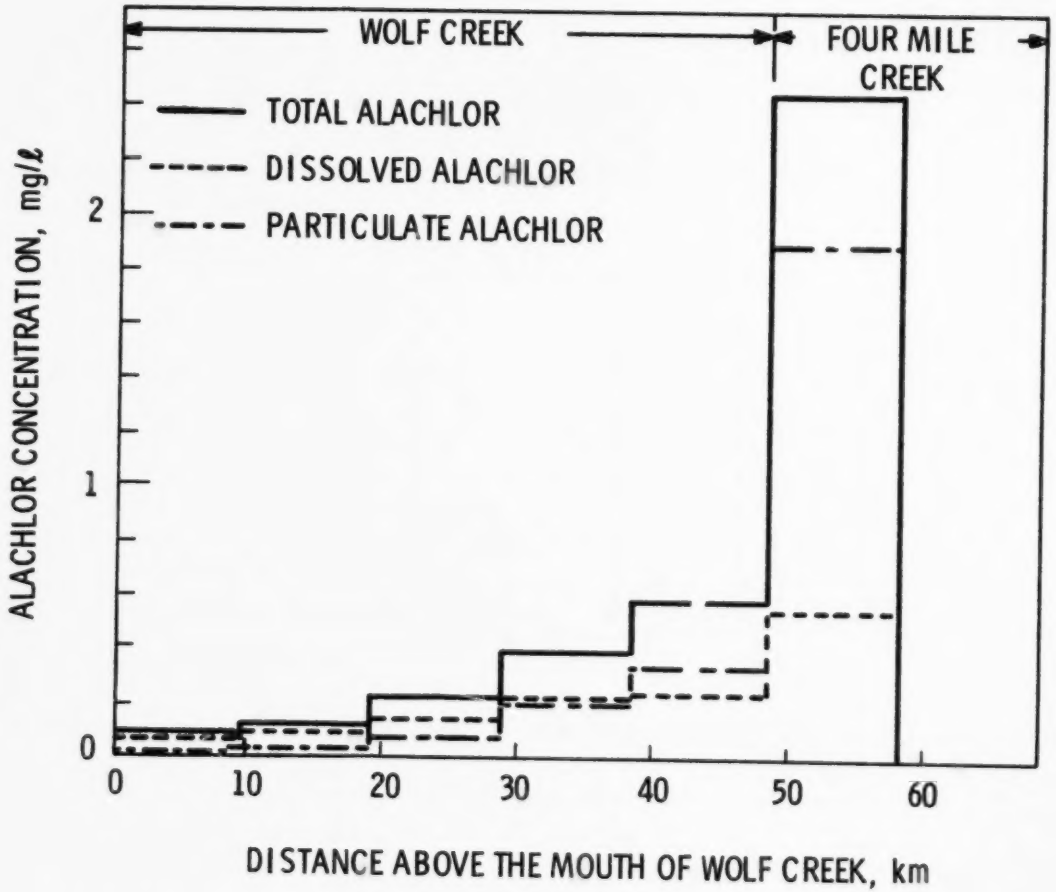

Figure 23. Longitudinal distributions of simulated dissolved, particulate and total alachlor at 6 a.m., June 4, 1973.

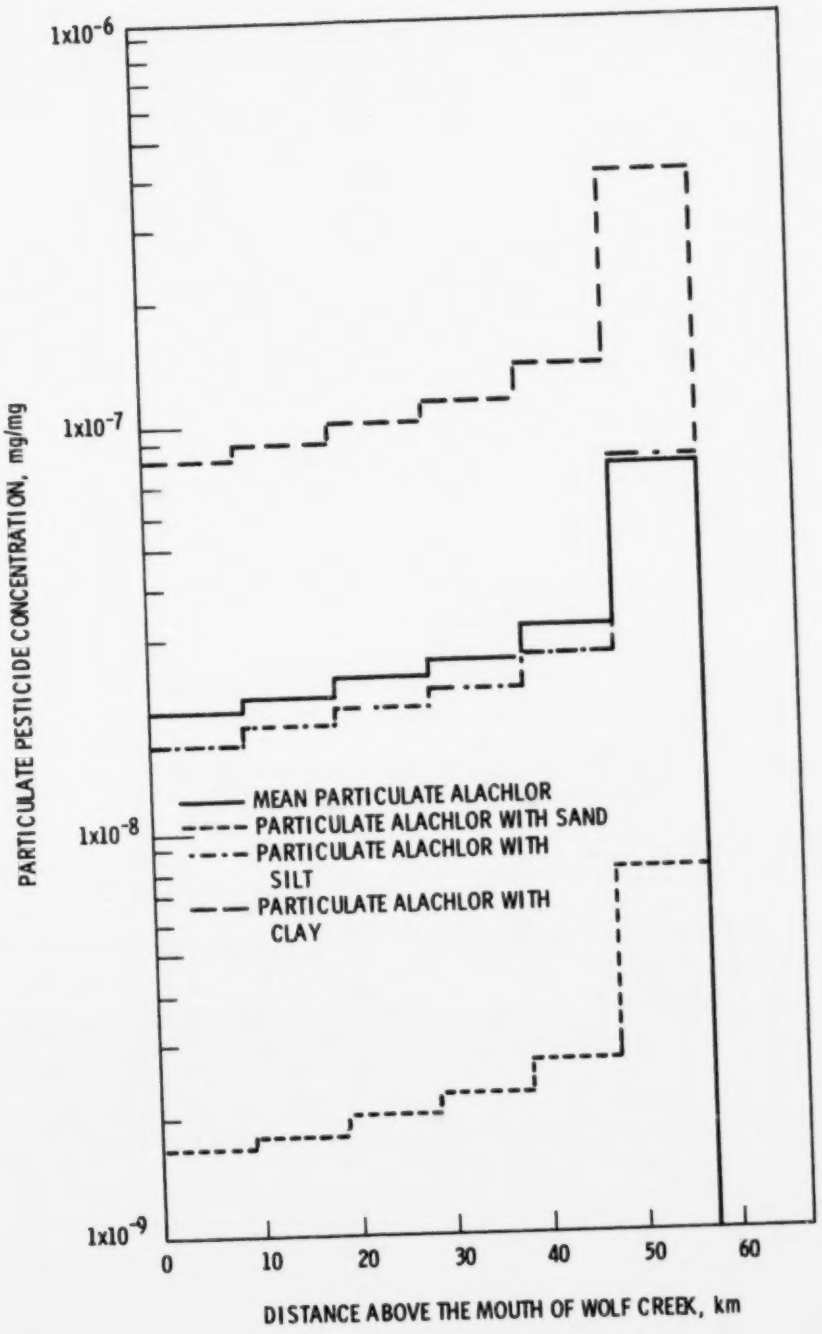

Figure 24. Variations of simulated particulate alachlor in the top bed layer accumulated during the three-year simulation period.

of sharp peaks associated with the high flows shown in Figure 8. Figures 10 and 11 indicate time variations of total particulate pesticide concentrations associated with sediments per unit weight of sediment and per unit volume of water, respectively. There are one large and several small peaks of particulate alachlor concentrations per unit weight of sediment (Figure 10) but only one large peak of particulate pesticide concentrations per unit volume of water (Figure 11). This is due to the fact that although alachlor concentrations attached to sediment per unit weight of sediment during the summer of 1972 are high, the sediment concentration during the same period is relatively low, so that the particulate alachlor concentration per unit volume of water becomes low. Dissolved and total (sum of dissolved and particulate) alachlor concentrations near the mouth of Wolf Creek are shown in Figures 12 and 13, respectively. There are one large and one small peaks of dissolved and total alachlor during the three-year simulation period. These simulation results revealed that high pesticide concentrations in the streams do not directly correlate with peak runoff or soil erosion events, but rather with the time between pesticide application and the first storm event after the application. In other words, pesticide concentrations in the stream have strong seasonal patterns (high peaks in May and June) corresponding to pesticide applications that were closely followed by precipitation causing runoff and soil erosion.

The results imply that the amount of pesticide being transported is controlled by the supply of pesticide on the land surface. Since alachlor degrades very rapidly after application to farm land, significant improvements in water quality can be obtained through the control and curtailment of both runoff and erosion shortly after pesticide application.

Instream modeling demonstrates some important effects of sediment transport on pesticide migration:

1. Through adsorption of dissolved pesticides by sediment, immediate biological availability of the pesticide may be reduced.

2. Through deposition of contaminated sediment, pesticide concentrations in a water column will be reduced.

3. However, the contaminated bed sediment then becomes a long-term source of pollution through resuspension and desorption.

Figure 8 through 13 clearly indicate a small number of sharp peaks of water discharge, sediment concentration, and concentrations of particulate, dissolved and total alachlor occurred during the three-year period. Comparison of Figures 11, 12 and 13 reveals that the majority of alachlor transported during May 1972 and June 1973 near the mouth of Wolf Creek was in a dissolved form due to the deposition of contaminated sediment before it reached the mouth of Wolf Creek. The dissolved pesticide distribution near the mouth of Wolf Creek shown in Figure 12 was then statistically analyzed by the program FRANCO to obtain the frequency of occurrence and duration of given pesticide concentrations, which were then used to evaluate the potential acute and chronic impacts of the pesticide to aquatic biota (Onishi et al. 1979b and Olsen and Wise 1979).

More detailed flow rates, sediment concentrations, and concentrations of particulate, dissolved and total alachlor near Wolf Creek mouth for the two high flow periods during the simulation period are shown in Figures 14 through 21. The highest predicted alachlor concentrations during the three-year period occurred on June 5, 1973. Figure 21 reveals that when the predicted maximum alachlor concentration occurred near the mouth of Wolf Creek on June 5, 1973, sediment carries only approximately 35% of the total alachlor, while 65% was transported as a dissolved form.

Predicted longitudinal distributions of sediment concentration and concentrations of dissolved, particulate and total alachlor occurring on June 5, 1973, are presented in Figures 22 and 23, respectively. Predicted longitudinal alachlor distribution in the top bed layer after the 3-year simulation is shown in Figure 24. Since initially it was assumed that there was no alachlor in the stream bed, Figure 24 shows the predicted accumulation of alachlor in the bed occurring during the three-year period.

Unfortunately, there are no measured data available to examine the accuracy of model predictions.

REFERENCES

Baca, R. G., W. W. Waddel, C. R. Cole, A. Brandstetter and D. B. Cearlock. "EXPLORE-I: A River Basin Water Quality Model," Battelle, Pacific Northwest Laboratories, Richland, WA.

Baker, J. L., H. P. Johnson, M. A. Borcherding, and W. R. Payne. 1979. "Nutrient and Pesticide Movement from Field to Stream: A Field Study," In Best Management Practices for Agriculture and Silviculture, Proceedings of the 1978 Connel Agricultural Waste Management Conference, Ann Arbor Science Publishers, Inc., Ann Arbor, MI.

Desai, C. S. and J. F. Abel. 1972. Introduction to the Finite Element Method, A Numerical Method for Engineering Analysis, Van Norstrand Reinhold Company, New York.

Falco, J. W., K. T. Sampson, and R. F. Carsel. 1976. "Physical Modeling of Pesticide Degradation," Proceedings of Symposium on Model Ecosystem Approach to Biodegradation Studies, Society for Industrial Microbiology, held in Jekyll Island, GA, pp. 193-202.

Krone, R. B. 1962. Flume Studies of the Transport of Sediment in Estuarial Shoaling Processes. Hydraulic Engineering Laboratory and Sanitary Engineering Research Laboratory, University of California at Berkeley.

Leendertse, J. A. 1970. A Water Quality Simulation Model for Well Mixed Estuaries and Coastal Seas, Principles of Computation, Volume I, RM-6230-RC, The Rand Corp., Santa Monica, CA.

Mahmood, K. and V. M. Ponce. 1975. Computer Programs for Sediment Transport--Documentation and Listing, CER75-76 KM-VMP2, Engineering Research Center, Colorada State University, Fort Collins, CO.

Norton, W. R., I. P. King, and G. T. Orlob. 1973. A Finite Element Model for Lower Granite Reservoir, Water Resources Engineers, Inc., Walnut Creek, CA.

Norton, W. R., L. A. Roesner, D. E. Evenson, and J. R. Monser. 1974. Computer Program Documentation for the Stream Quality Model, Qual-II, Water Resources Engineers, Inc., Walnut Creek, CA.

Olsen, A. R. and S. E. Wise. 1979. Frequency Analysis of Pesticide Concentrations for Risk Assessment, Battelle, Pacific Northwest Laboratories, Richland, WA.

Onishi, Y., P. A. Johanson, R. G. Baca, and E. L. Hilty. 1976. Studies of Columbia River Water Quality--Development of Mathematical Models for Sediment and Radionuclide Transport Analysis. BNWL-B-452, Battelle, Pacific Northwest Laboratories, Richland, WA.

Onishi, Y. 1977. Mathematical Simulation of Sediment and Radionuclide Transport in the Columbia River. BNWL-2228, Battelle, Pacific Northwest Laboratories, Richland, WA.

Onishi, Y. 1979a. "Evaluation of Mathematical Models of Hazardous Substances on Surface Waters," Proceedings of the U.S. Environmental Protection Agency's National Workshop of Verification of Water Quality Models, West Point, NY.

Onishi, Y. 1979b. User's Manual for EXPLORE-I: A River Basin Water Quality Model (Hydraulic Module Only). Submitted to U.S. Environmental Protection Agency by Battelle, Pacific Northwest Laboratory, Richland, WA.

Onishi, Y. and S. E. Wise. 1978. "Mathematical Modeling of Sediment and Contaminant Transport in the James River Estuary," Proceedings of the 26th Annual ASCE Hydraulics Division Specialty Conference on Verification of Mathematical and Physical Models in Hydraulic Engineering, College Park, MD, pp. 303-310.

Onishi, Y. and S. E. Wise. 1979. User's Manual for the Instream Sediment-Contaminant Transport Model, SERATRA, Battelle, Pacific Northwest Laboratories, Richland, WA.

Onishi, Y., D. L. Schreiber, and R. B. Codell. 1979a. "Mathematical Simulation of Sediment and Radionuclide Transport in the Clinch River, Tennessee," Proceedings of ACS/CSJ Chemical Congress, Honnolulu, Hawaii, April 2-7, 1979, Contaminants and Sediment, edited by R. A. Baker, Ann Arbor Publisher, Inc.

Onishi, Y., S. M. Brown, A. R. Olsen, M. A. Parkhurst, S. E. Wise, and W. H. Walters. 1979b. Methodology for Overland and Instream Migration and Risk Assessment of Pesticides, Battelle, Pacific Northwest Laboratories, Richland, WA.

Partheniades, E. 1962. A Study of Erosion and Deposition of Cohesive Soils in Salt Water. Ph.D. Thesis, University of California at Berkeley.

Smith, J. H., W. R. Mabey, N. Bohonos, B. R. Holt, S. S. Lee, T. W. Chon D. C. Bomberger, and T. Mill. 1977. Environmental Pathways of Selected Chemicals in Freshwater Systems, EPA-600/7-77-133, SRI International, Menlo Park, CA, Submitted to EPA Environmental Research Laboratory, Athens, GA.

Stanford Research Institute. 1979. "Fate of Selected Pollutants -- Protocall II." Photolysis in Water. U.S. Environmental Protection Agency, Contract Number 68-03-2227.

Tofflemire, T. J., S. O. Quinn, and P. R. Hague. 1979. PCB in the Hudson River - Mapping, Sediment Sampling and Data Analysis, Technical Paper No. 57, Department of Environmental Conservation, the State of New York.

U.S. Environmental Protection Agency. 1978. Kepone Mitigation Project Report, Standard and Criteria Office of Water and Hazardous Materials, Washington DC.

Vanomi, V. A., Editor. 1975. Sedimentation Engineering. Prepared by the ASCE Task Committee for the Preparation of the Manual on Sedimentation of the Sedimentation Committee of the Hydraulics Division, New York, NY.

Varga, R. S. 1965. Matrix Iterative Analysis, Prentice-Hall, Inc.

Zepp, R. G. and D. M. Cline. 1977. Rates of Direct Photolysis in Aquatic Environments. Environ. Sci. Technol. 11:359-366.

U.S. GOVERNMENT PRINTING OFFICE: 1982—559-092/468